Ketoacids as antioxidants in human astrocytes exposed to oxidative and aluminum stress.

Sean Thomas

An undergraduate thesis submitted to the Department of Chemistry/Biochemistry at

Laurentian University

In partial fulfillment for an Honours Bachelor of Science degree in Biochemistry.

Approved by:

Supervisor: _____ Date: _____

Second Reader: _____ Date: _____

Abstract

Aluminum (Al), the most abundant metal in the earth's crust, has been implicated in a number of neurological diseases. Its increased bioavailability has been associated with increased toxicity in humans. Increased lipid accumulation occurs as a result of disruption in carnitine homeostasis due to the shunting of α-ketoglutarate (αKG) towards reactive oxygen species (ROS) detoxification. The purpose of this study was to elucidate the role of ketoacids such as oxaloacetate (OAA) and αKG in combating oxidative stress in astrocytes. The present study has shown the ability of ketoacids such as αKG and OAA to sequester ROS in the astrocytes and restore normal lipid levels as observed through fluorescence microscopy. The non-enzymatic decarboxylation of αKG and OAA into succinate and malonate respectively as observed in the HPLC studies point to the role of these ketoacids in ROS detoxification. Furthermore, the tricarboxylic acid (TCA) cycle activity which is diminished under oxidative stress as gauged by the activity of NAD-ICDH, was found to be restored to normal levels in the stressed cells upon recovery with OAA. Expression of apolipoprotein E, an essential biomolecule in lipid and β-amyloid metabolism, was found to be down-regulated under aluminum stress, an observation that was reversed by OAA recovery. Hence it appears that the ketoacids play a critical role in quelling ROS in human astrocytes.

Acknowledgements

There are several people to whom I owe eternal gratitude for their help and support through all the years of my undergraduate studies. First and foremost, I thank my co-supervisors, Dr. Appanna, Dr. Omri & Dr. Chahma. To Dr. Appanna, for giving me a research position, and trusting me with a eukaryotic project, thank you very much. Beyond the guidance with the project, the passion for research that you instilled in me is something I shall cherish forever. To Dr. Omri and Dr. Chahma, for taking the time to carefully look over all the details and providing invaluable feedback about my research, that helped shape and improve it, thank you very much. For making this an incredible learning experience and all the help and guidance in understanding the work, I am truly grateful.

To the people in my lab, namely Adam, Azhar, Chris, Joe, Sungwon, Varun, and Zach, I thank you for your help and for making the lab the best place to work in. Special thanks go out to Zachary Castonguay for teaching me practically everything I know about astrocytes and who sacrificed much of the time he should have dedicated to his own thesis to help me with mine. Truly appreciate it. I would like to thank Christopher Auger and Dr. Joseph Lemire for being phenomenal lab managers and bringing an enthusiasm to the lab that made even the most depressing days great. The vast amount of knowledge I gained from both of you about practical matters in research is one of the most important lessons I've learnt at university. Last but certainly not least, I wish to thank Sungwon for the years of academic advice, guidance and friendship. Thanks a lot!

To all my professors here at Laurentian, I would like to say heartfelt thanks for taking the time to train our minds. We learnt a great deal from you. I would also like to

thank all the lab technicians who've helped hone my laboratory skills especially, Pieter, Paul and Bernie. Thank you very much.

On a more personal note, I owe my deepest gratitude to my grandparents, my entire family and especially my parents, who have sacrificed a lot for my brother and me and whom I love more than anything in this world. I would also like to thank my brother because if I were Fred, he'd be my George and I really can't imagine what I would have done without him. I also feel greatly obliged to thank all of the teachers who have ever taught me, from Mrs. Weatherall and Mrs. Khodai in my preschool years to Ms. Kavitha, Mr. Barry and Mr. Urso in my high school years, for making me the student I am.

Though I thank each and every one of my friends for their friendship and the happiness they brought into my life, I need especially to thank Michael Keller because I would never have been able to do half the things I did without his help throughout my grade 12 and university years. Among others, I would like to thank Bradley Brisson for showing me that life is made far more beautiful by the friends we have in them. I would also like to thank Dayna Corelli for teaching me an important lesson about life: to go wherever I go, with all my heart. And finally, I would like to thank Radhika Bhaskar because there are moments in life that define you, where character is forged. For all the help through those times, thank you! Lie readily, Volcano!!!

Table of Contents

Abstract 2

Acknowledgements 3

List of Figures/tables/schemes 7

List of abbreviations 8

Introduction 11

1.1 Biochemistry of the brain 11

1.2 Structural role of astrocytes. 12

1.3 Astrocytes and neurotransmitter clearance 13

1.4 Astrocytes, lipids cholesterol and Apolipoprotein E 15

1.5 Astrocytes & Oxidative Stress 17

1.5.1 Astrocytes and ROS 17

1.5.2 Astrocytes and Al 18

1.5.3 ROS detoxification 19

1.6 Ketoacids 20

1.6.1 Ketoacids as therapeutic agents 20

Thesis Objectives 24

Materials and Methods 25

2.1 List of reagents and equipments 25

2.2 Cell Culturing 26

2.3 Cell isolation and spent fluid collection 29

2.3.1 Mitochondrial isolation 29

2.4 Bradford Assay 30

2.5 Native polyacrylamide gel electrophoresis 30

2.5.1 Sample preparation 30

2.5.2 Native Gel preparation 31
2.5.3 In-gel enzyme assays and protein expression 32
2.6 Fluorescence microscopy 34
2.6.1 Culture growth 34
2.6.2 Fixing the slides 35
2.7 High Performance liquid chromatography (HPLC) studies 36
Results 38
3.1 Lipid homeostasis under stress and the effects of ketoacid recovery 38
3.2 The involvment of OAA in recovering mitochondrial activity 39
3.3 Disruption and restoration of L-carnitine levels upon OAA recovery 41
3.4 Monitoring ROS levels under stress and OAA recovery 42
3.5 Comparing the malonate levels before and after OAA recovery 43
3.6 Delineating the role of succinate production in ROS detoxification 44
3.7 Blue Native Polyacrylamide Gel Electrophoresis for NAD-ICDH 45
3.8 Western blot for apolipoprotein E expression 46
Discussion 47
Conclusion 52
References: 53

List of Figures/tables/schemes

List of figures

Figure 1: Overview of organization of the brain cells 12
Figure 2: Isolation of synaptic cleft by astrocytes 13
Figure 3: Astrocyte Neuron Lactate shuttle and Glu/Gln shuttle 14
Figure 4: Role of ApoE in cholesterol regulation and Aβ degradation 16
Figure 5: Free radical generation from molecular oxygen 17
Figure 6: ROS Production as a result of free floating iron and copper 18
Figure 7: NAD-ICDH activity as gauged through BN-PAGE 19
Figure 8: ROS levels monitored using DCFH-DA fluorescence microscopy 22
Figure 9: Disruption of lipid homeostasis under ROS 23
Figure 10: Overview of cell culturing 28
Figure 11: In-gel detection of NAD(P) dependent enzymes 33
Figure 12: Overview of cell culturing for microscopy 35
Figure 13: Lipid levels as observed by Oil red O microscopy 39
Figure 14: Comparison of mitochondrial activity using rhodamine staining 40
Figure 15: Analysis of carnitine levels under stress and upon OAA recovery 41
Figure 16: Detecting ROS levels using DCFH-DA staining 42
Figure 17: Exploring malonate levels as a by-product of ROS detoxification 43
Figure 18: Evaluating succinate production as a mode of ROS sequestration 44
Figure 19: Evaluating NAD-ICDH activity upon recovery with OAA 45
Figure 20: Confirmation of NAD-ICDH bands using HPLC 46
Figure 21: ApoE expression under stress and after OAA recovery 46

List of tables

Table 1: Bradford Assay preparation 31
Table 2: Recipe for 4-16% Blue Native Polyacrylamide gel 33

List of abbreviations

AD	Alzheimer's disease
αKG	Alpha ketoglutarate
Al	Aluminum
Asp	Aspartate
α-MEM	Apha-minimum Eagle media
BDH	β- hydroxybutyrate dehydrogenase
BHB	β- Hydroxybutyrate
BN	Blue Native
CNS	Central Nervous system
CS	Citrate Synthase
CSB	Cell storage Buffer
DMSO	Dimethyl Sulphoxide
FA	Fatty Acid
FBS	Fetal Bovine Serum
g	gram

Glu	Glutamate
Gln	Glutamine
GS	Glutamine synthase
GSH	Glutathione
HD	Huntington's disease
HMG-CoA	3 hydroxy 3 methylglutaryl CoA
Hr(s)	hour(s)
INT^O	Iodonitro Tetrazolium salt (oxidized)
INT^R	Iodonitro Tetrazolium salt (reduced)
L	Liter
MCT	Monocarboxylate transporter
mL	milliliter
min	minute
mM	Millimolar
NAD+	Nicotinamide adenine dinucleotide (oxidized form)
NADH	Nicotinamide adenine dinucleotide (reduced form)
NR cells	Non-recovered cells

OAA	Oxaloacetate
OS	Oxidative stress
PAGE	Polyacrylamide Gel electrophoresis
PBS	Phosphate buffered Saline
PMS^{O}	Phenazine Methosulfate (oxidized)
PMS^{R}	Phenazine Methosulfate (reduced)
PD	Parkinson's disease
ROS	Reactive oxygen species
Sec	seconds
TCA	Tricarboxylic acid cycle
V	Volt

Introduction

1.1 Biochemistry of the brain

The human brain is not a book to be opened at will and examined at leisure. The anatomy and physiology of the brain is a complex and many-layered phenomena that researchers are only beginning to understand. Although the brain only accounts for about 2% of the body's mass, it consumes about 18-20% of the body's energy reserves, making it the most energy demanding organ of the body (Martini & Ober, 2006) (Guzman & Blazquez, 2001). Also, the brain consumes 20-50% of the available arterial blood O_2, making it one of many organs such as the heart, liver, etc. to be heavily dependent on oxidative metabolism (Martini & Ober, 2006). Although most of the energy is utilized by the neurons in the brain for the continuous propagation of action potentials, a great deal of energy is expended on supportive tissues including oligodendrocytes, ependymal cells, microglia, and astrocytes (Martini & Ober, 2006).

Each of the supporting cells plays a specific role within the brain. Microglia are typically involved in the brain for immunity whereas oligodendrocytes serve to insulate neurons through the formation of myelin sheaths (Martini & Ober, 2006) (Siegel, 2006). Ependymal cells tend to line the cavities of the central nervous system (CNS) and form the cerebral spinal fluid which they then circulate using their cilia. Astrocytes orient themselves in the brain to allow for the complex interaction with neurons (figure 1). Also, astrocytes mediate metabolite flow between neurons and vascular endothelia (the blood supply). Since astrocytes outnumber all other cell types within the brain, they play the most important role in the brain in terms of structural support and brain metabolism (Martini & Ober, 2006) (Magistretti & Pellerin, 1999).

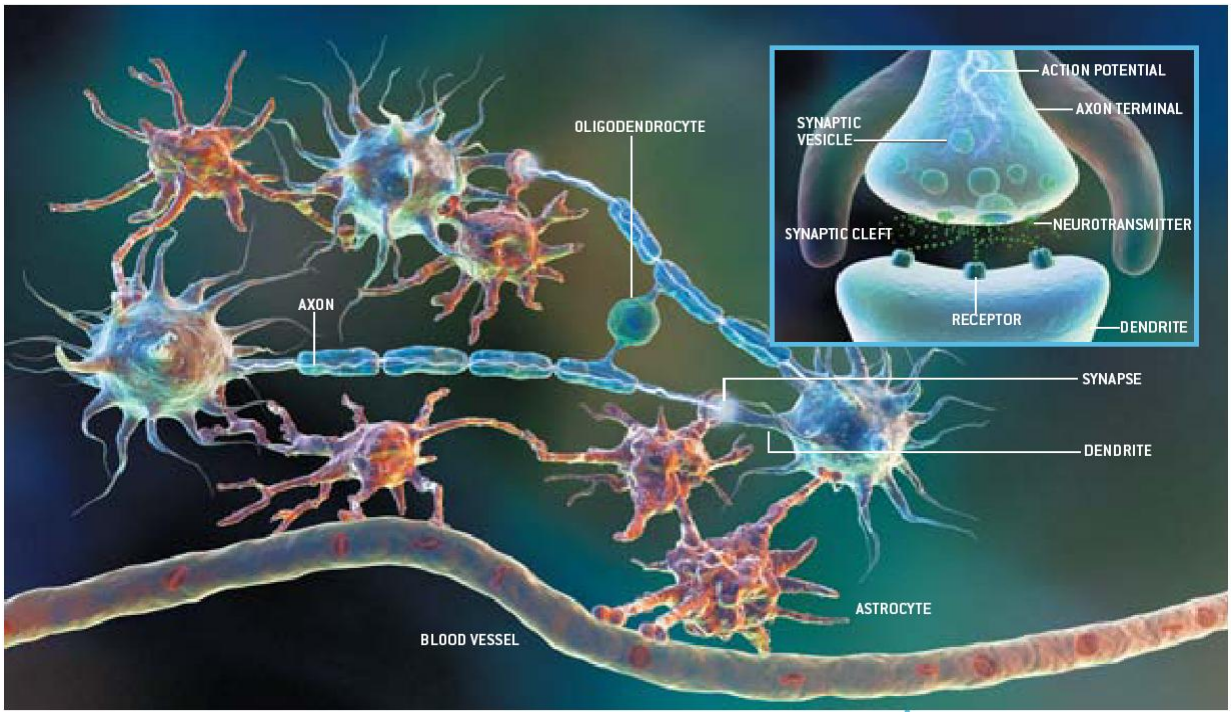

Figure 1: Overview of organization of the brain cells. Astrocytes are the most numerous cells and provide an interface between the blood vessels and neurons. They also provide structural support and perform a wide variety of other functions. (R. Douglas Field, Sci. Am., April 2004)

1.2 Structural role of astrocytes.

Present research has shown that astrocytes outnumber neurons in the CNS at a ratio of 9:1 (Magistretti & Pellerin, 1999). The long cellular projections on the astrocytes are called end-feet or filopodia. Astrocytes use their filopodia to insulate the synaptic cleft (space between the post-synaptic and pre-synaptic neuron) by wrapping around it and thereby isolating it (figure 2) (Barker & Ullian, 2010). By isolating the synaptic cleft, the astrocytes are able to ensure that misfiring of action potentials do not occur.

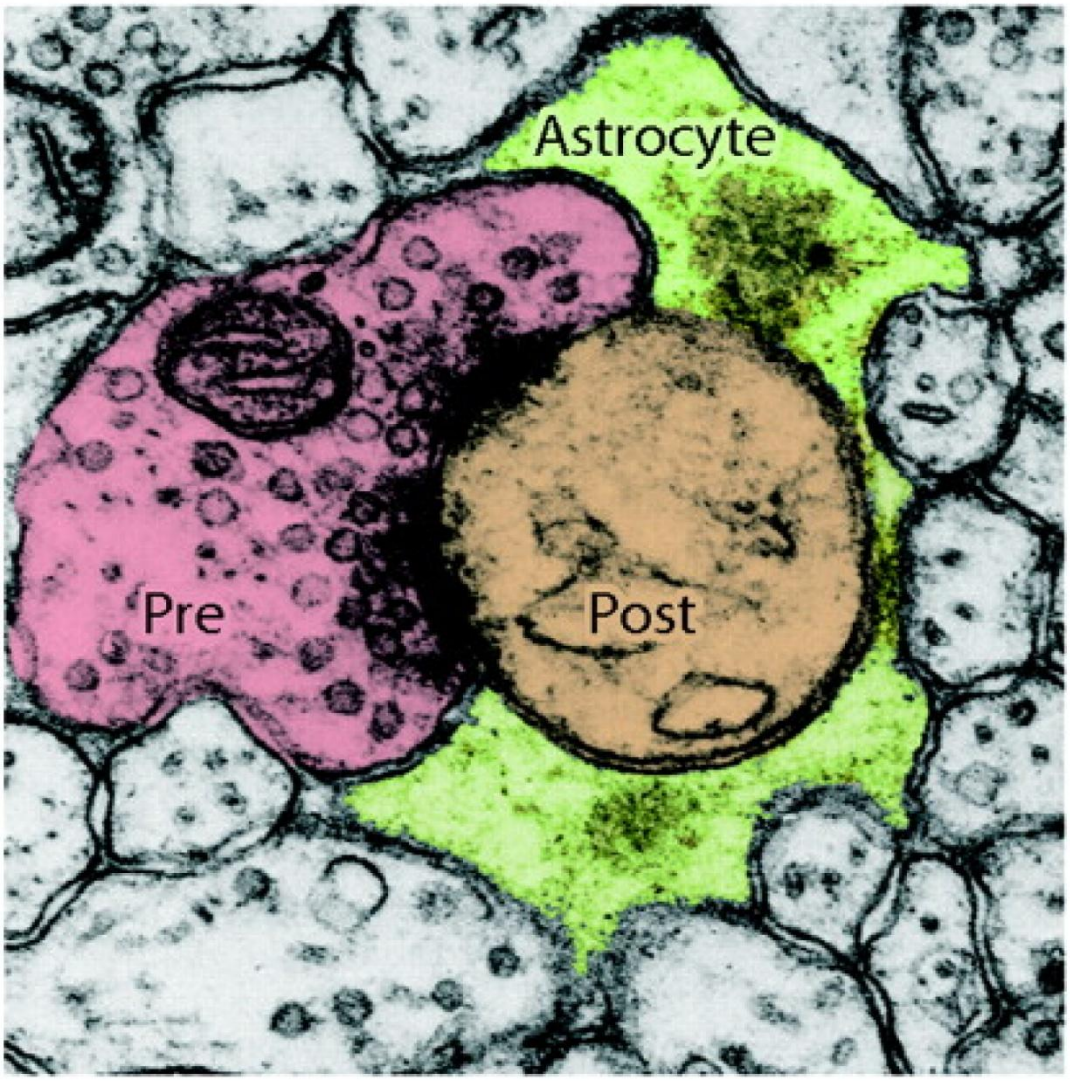

Figure 2: Isolation of synaptic cleft by astrocytes (Fellin et al., Physiology 21, 208 (2006)

1.3 Astrocytes and neurotransmitter clearance

Of the many important roles that astrocytes play in the human brain, neurotransmitter clearance is probably the most important. Most neurons in the brain utilize Glutamate (Glu) as their neurotransmitter. Thus 80-90% of the synapses in the brain are thought to be glutamatergic (Lazarowski et al., 2003). Astrocytes function to remove any excess Glu from

the synaptic cleft following neurotransmission and convert it to glutamine (Gln) prior to sending it back to the neurons where it is reconverted into Glu as per the Glu/Gln shuttle (figure 3) (Attwell & Laughlin, 2001) (Walton & Dodd, 2007). Glutamatergic activity is thought to account for 80% of the energy metabolism within the brain (Attwell & Laughlin, 2001). In addition to energy production from the neurons, the high energy demand of its functioning means that the neurons depend heavily on astrocytes to supplement the neurons with the excess energy. This is accomplished by the neuron astrocyte lactate shuttle for the supplementation of the huge energy demands of the neurons. Glucose entering the astrocytes undergoes anaerobic metabolism within the narrow filopodia of the astrocytes to form lactate which is then used to supplement the oxidative metabolism in the surrounding neurons (figure 3). The lactate is extremely important as a neuronal metabolic substrate for the sustenance of the intense neuronal activity (Yudkoff et al., 2007).

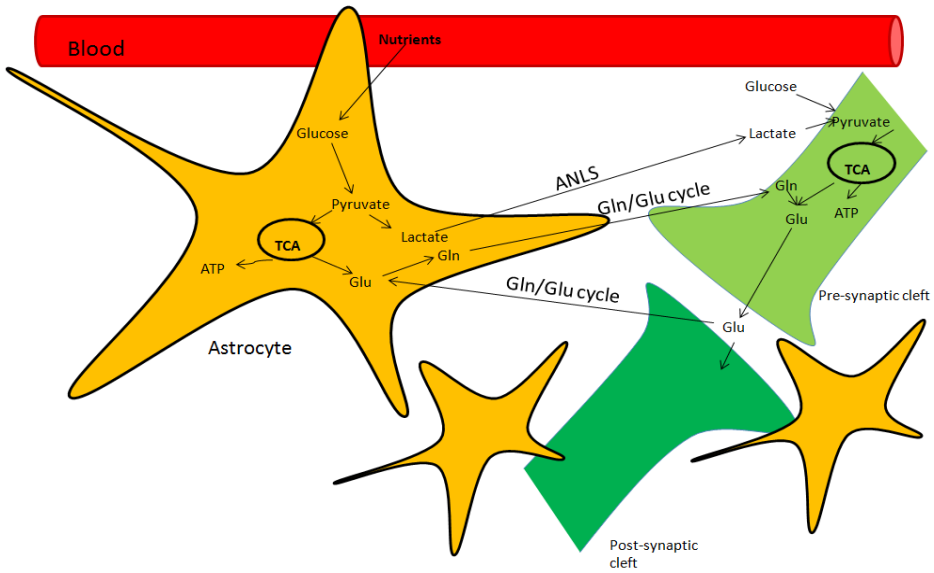

Figure 3: Astrocyte Neuron Lactate shuttle and Glu/Gln shuttle

1.4 Astrocytes, lipids cholesterol and Apolipoprotein E

Although the brain is composed of 50% lipids in dry weight, the mechanisms of lipid metabolism and trafficking within the brain are not very well understood (Siegel, 2006). Lipids in the brain are used for the formation of neural and astroglial processes as well as myelination of the axons, which is required for the propagation of action potentials (Siegel, 2006). Lipid synthesis is typically taken care of by oligodendrocytes. However astrocytes play a key role in lipid metabolism by regulating levels of cholesterol, apolipoprotein E, and specialized fatty acids. Apolipoprotein E which is almost exclusively formed within astrocytes in the brain, functions as a cholesterol and phospholipid carrier within the brain (Pfrieger, 2003). Misregulation of apoE has been found to lead to Aβ-Peptide accumulation which in turn has been implicated in Alzheimer's disease (figure 4) (Pfrieger, 2003). Since neurons are unable to synthesize their own cholesterol they depend heavily on astrocytes for their supply of cholesterol.

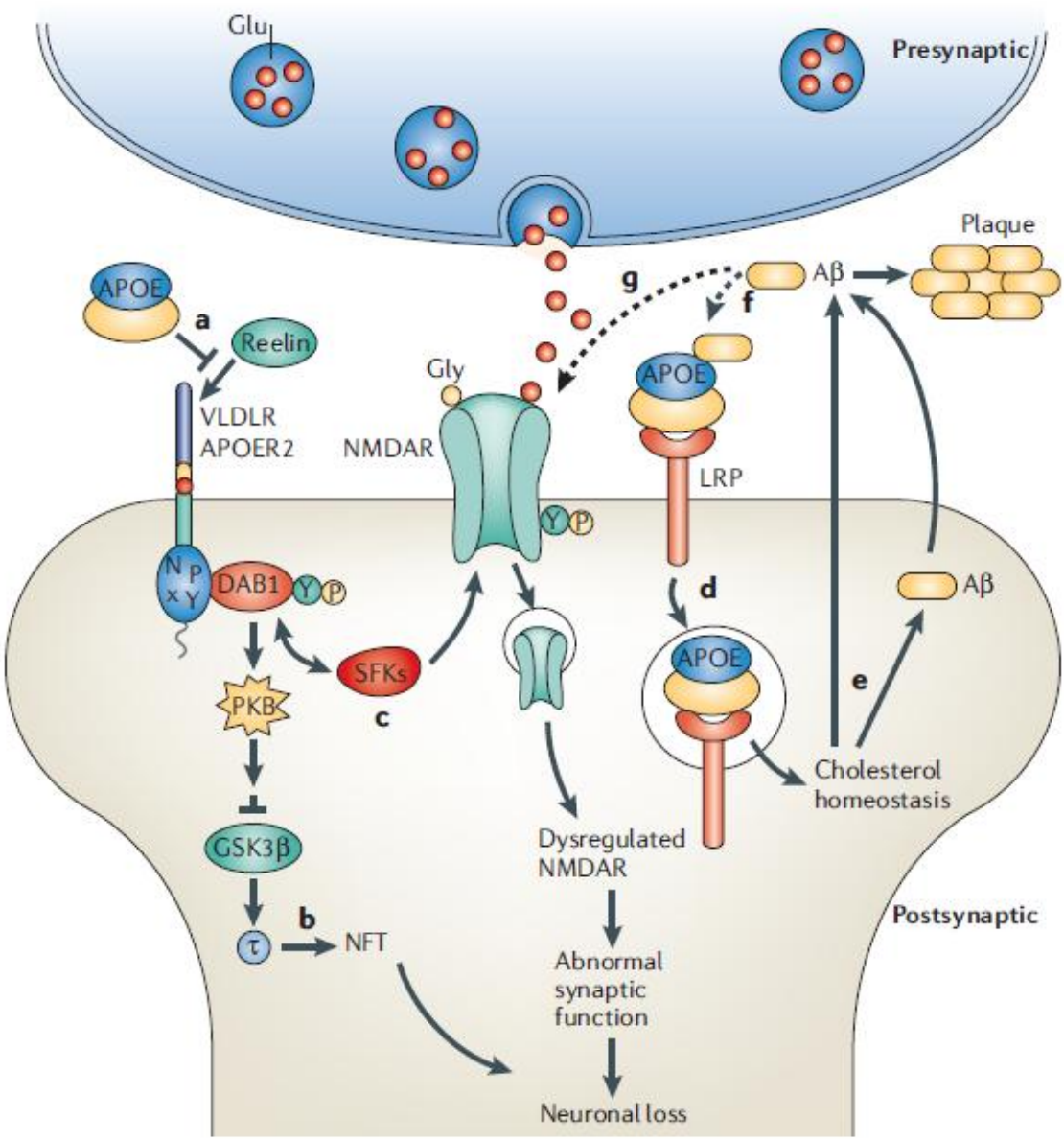

Figure 4: Role of apoE in cholesterol regulation and Aβ degradation (Herz & Chen, *Nature*, 2006)

Although studies of neurodegenerative diseases and other brain-related diseases have typically focused on neurons, it is important to note that astrocytes play an almost equally important role by providing structure, metabolic support, neurotransmitter clearance, cholesterol production and essential fatty acid synthesis for neurons to be able to perform

their job of neurotransmission (Lemire et al, 2009). Thus, studying astrocytes and the effects of toxicants on astrocytes is probably just as important as studying these effects on neurons (Schell et al, 1995).

1.5 Astrocytes & oxidative Stress

To supply the neurons with the energy required for their activity, the neurons and astrocytes show heightened oxidative metabolism. Increased usage of O_2 during this process has been shown to lead to increased production of ROS (Kimura & Kimura, 2004). Within cells at low levels, ROS have shown to perform a wide variety of functional roles including hypoxic signalling, physiological redox signalling, etc. However, at elevated levels, it can lead to cell death through apoptotic signalling or necrosis. (Kimura & Kimura, 2004).

1.5.1 Astrocytes and ROS

Oxygen can undergo singlet electron reduction to form a wide variety of harmful ROS (figure 5). One of the most common uses of ROS is by phagocytic cells and neurtrophils in killing invading microbes. These cells utilize NADPH oxidase to generate superoxide ions ($O_2^{\cdot-}$) by reducing O_2 using NADPH as the electron donor (Babior, 1999)

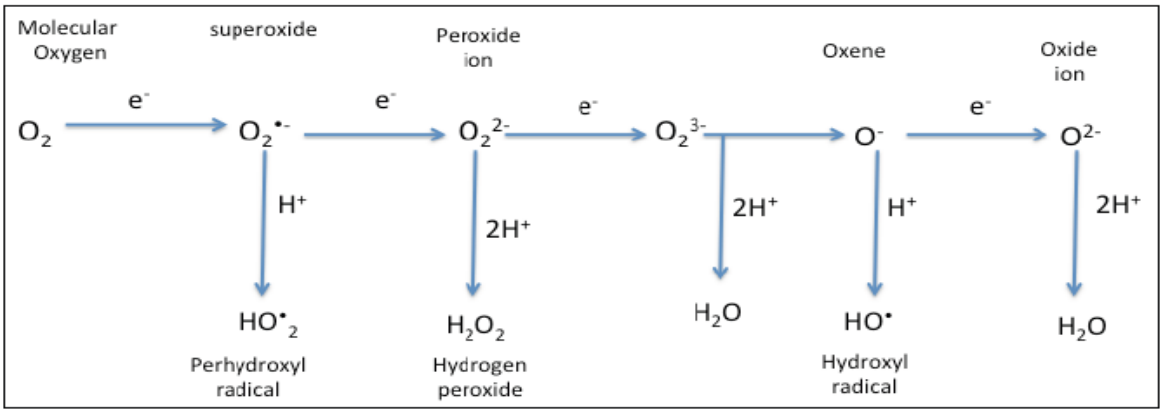

Figure 5: Free radical generation from molecular oxygen (Lemire, 2011)

Research suggest that 2-5% of all of the O_2 utilized by the electron transport chain (ETC) undergoes incomplete reduction by electron leakage resulting in higher levels of ROS. Also, free iron and copper can lead to the production of hydroxide ions via the Fenton reaction and Haber-Weiss reactions (figure 6) (Lemire, 2011).

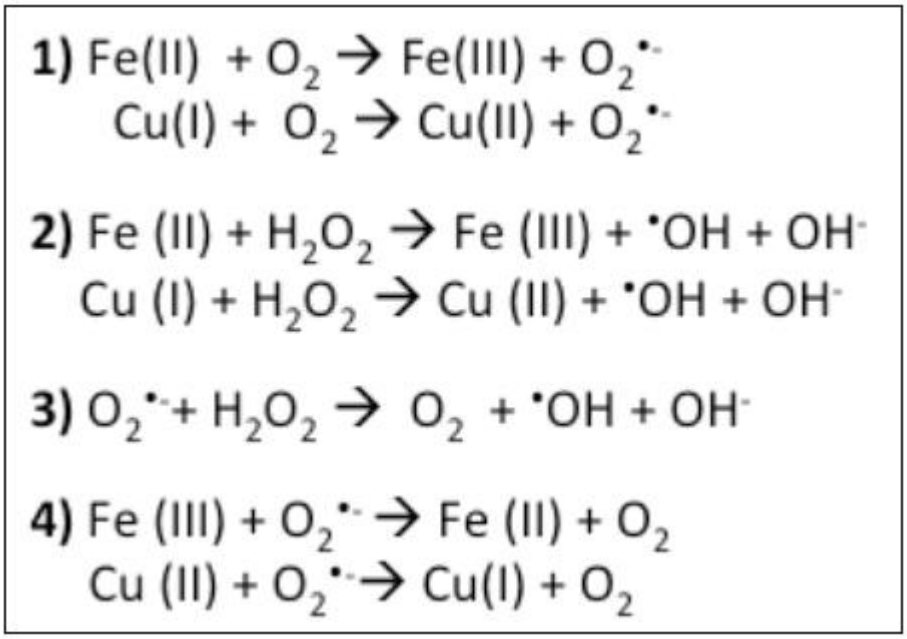

Figure 6: ROS Production as a result of free floating iron and copper. (Lemire, 2011)

A comparatively newly studied mechanism of ROS generation is through the displacement of Fe^{3+} molecules by aluminum toxicity.

1.5.2 Astrocytes and Al

Aluminum exists predominantly in its Al^{3+} state. As such, in high amounts, it tends to displace Fe^{3+} molecules leading to the generation of ROS. Within astrocytes, aluminum toxicity has also been shown to reduce ATP production via down regulation of the ETC as

well as the TCA cycle as seen through the down regulation of NAD-ICDH, a key marker of TCA cycle activity (figure 7) (Lemire et al, 2008).

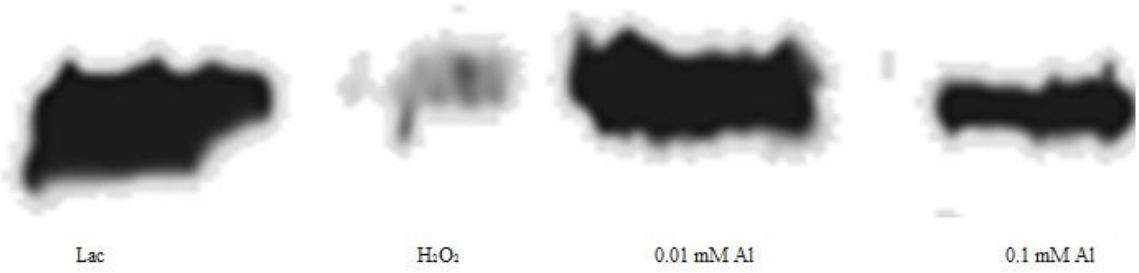

Figure 7: NAD-ICDH activity as gauged through BN-PAGE. (Lemire et al., 2008, *J Neurosci Res87:* 1474-1483)

Al also exerts its toxic effects by disrupting the lipid bilayer. This is accomplished by the binding of Al to the oxygen-rich hydrophilic tails of phospholipids which in turn exposes the hydrophobic tails to the ROS that is generated within the cells. The findings of Al in the histological hallmarks of AD and PD suggests that the metal probably plays some role in the pathogenesis of these disorders (Zhu et al, 2007).

1.5.3 ROS detoxification

Cells have evolved specialized mechanisms for ROS detoxification when their levels become too high. The cell's classical non-enzymatic anti-oxidant defense mechanisms utilize biological macromolecules such as vitamin C (Ascorbic acid), vitamin E (α-tocopherol), arginine, glutathione, etc. (Fang et al., 2002). Glutathione (GSH), a tripeptide composed of glutamate, cysteine and glycine, is present in vast amounts in specialized tissues such as brain, liver, heart, and muscles due to its ability to sequester ROS and at the same time generate in excess, the anabolic reducing agent NADPH via the pentose

phosphate pathway. NADPH is required for the reactivation of enzymes such as catalase described below. Thus GSH, in conjunction with other molecules and enzymes, couples the non-enzymatic anti-oxidant defense system to the enzymatic anti-oxidant defense system.

Enzymatically, superoxide radicals are detoxified using the enzyme superoxide dismutase (SOD), which catalyzes the disproportionation of $O_2^{\cdot-}$ to H_2O_2 and O_2. H_2O_2 is then sequestered using the enzyme catalase which converts H_2O_2 into H_2O and O_2 (Fang et al, 2002). Present research suggests the possibility of utilizing α-ketoacids in ROS sequestering.

1.6 Ketoacids

The human body consists predominantly of three ketoacids, namely, pyruvate, αKG and OAA (Maalouf et al, 2007). Ketoacids play an important role in most central metabolic pathways. Their ability to scavenge reactive oxygen species (ROS) and their natural occurrence within the body has made them a prime target for future clinical therapy (Maalouf et al., 2007).

1.6.1 Ketoacids as therapeutic agents

Patients with severe burns were enterally fed ornithine αKG and it was found that the ornithine αKG supplementation significantly shortened healing times. Also, since αKG is a naturally occurring metabolite, its administration was found to be safe and well tolerated (Coudray-Lucas et al., 2000). It is believed that increasing age is one of the top risk factors for the prevalence of cataracts in patients with diabetes. The onset is believed to occur as a result of the formation of advanced glycation end products which are symptoms of the disease. However, research has shown that the ketoacids, pyruvate and αKG prevent the

formation of cataracts by competitively inhibiting the glycation reaction as well as acting as antioxidants (Varma et al., 1997).

In *P. fluorescens* as well as hepatocytes, αKG has been shown to scavenge ROS by utilizing an NADPH-independent pathway that leads to the production of succinate as well as CO_2 (Mailloux et al, 2008). In astrocytes, although the mechanism has not been delineated, lowering of ROS levels upon treatment with αKG has been established (figure 8).

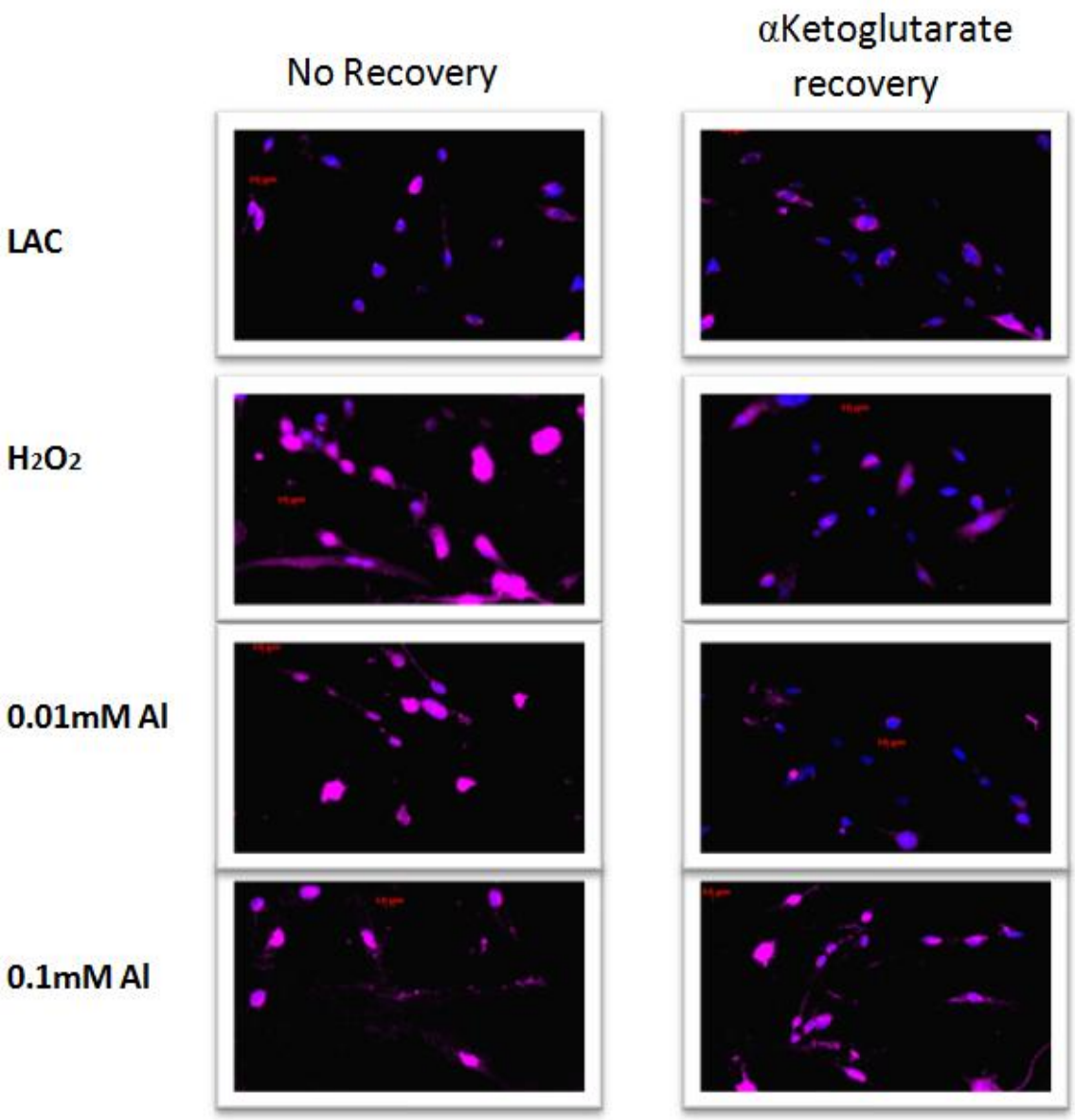

Figure 8: Sequestration of ROS using αKG as seen through DCFH-DA fluorescence microscopy. Cells were stained with the Hoescht stain (nucleus- blue) and DCFH-DA stain (ROS-purple) (Lemire et al., 2011, *Toxicology letters*, doi:10.1016/j.toxlet.2011.03.019)

Unfortunately, loss of free αKG during ROS sequestration has been linked to misregulation of lipid homeostasis. This has been shown to result from the lowered availability of αKG for the production of L-carnitine which is a moiety necessary for the

translocation of lipids to the mitochondria where it can then undergo β-oxidation (Lemire et al, 2011). This disruption of lipid homeostasis has been linked to increased lipid accumulation in cells which has been highly correlated to pathological conditions such as AD, PD, etc. Figure 9 summarizes the adverse effects of lowered αKG levels during OS. Research has shown the ability of αKG supplementation within astrocytes to restore carnitine levels to normal (Lemire et al, 2011).

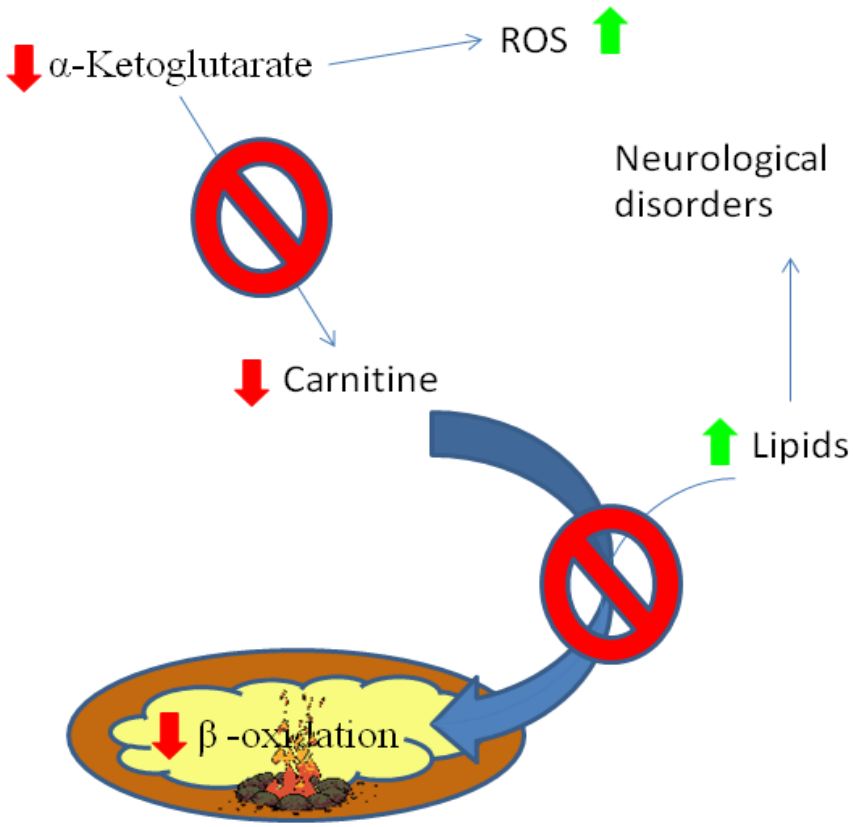

Figure 9: Disruption of lipid homeostasis under oxidative stress (OS). (Lemire et al, 2011, *Toxicology letters*, doi:10.1016/j.toxlet.2011.03.019)

Thesis Objectives

Neuronal metabolism is heavily dependent on astrocytes. Several neurological disorders such as AD, PD, etc. have been linked to oxidative stress and the presence of aluminum, a known pro-oxidant that has been established in the histological hallmarks of these diseases. Owing to the important role astrocytes play in supporting neuronal functioning, any H_2O_2 or Al-mediated alterations in astrocytic function could potentially prove fatal for the neurons and lead to neurodegeneration or cognitive decline.

The objective of this study was to investigate the antioxidant properties of the two ketoacids αKG and OAA in human astrocytes exposed to H_2O_2 as well as Al stress. The activity of NAD-ICDH, a key marker of TCA cycle activity was profiled using BN-PAGE. Lipid accumulation was also compared across all levels before and after recovery with the α-ketoacids. Levels of ROS were also monitored for the OAA-recovered cells and mitochondrial activity was monitored under conditions of stress vs. recovery. Using HPLC analyses, metabolite levels were gauged at to delineate the mechanism of ROS detoxification. Finally Western blot analysis was used to monitor apolipoprotein E expression.

Materials and Methods

2.1 List of reagents and equipments

- Sigma-Aldrich (St. Louis, Missouri)
  - αKG
  - Acetyl-CoA
  - Acrylamide
  - Ammonium persulfate
  - ATP
  - BSA
  - DCFHDA
  - Ferritin
  - Iodonitrotetrazolium Chloride
  - NAD (H)
  - Oil red O
  - OAA
  - Phenazine methosulfate
- Fisher Scientific (Unionville, Ontario)
  - Collagen coated cell culture flasks 175 cm^2, 75 cm^2
  - Fisher model 500 sonic dismembrator
  - HPLC grade monobasic potassium phosphate
  - Ultraspec 3100 Pro spectrophotometer
- Waters Ltd. (Mississauga, Ontario)
  - Alliance 2487 Dual wavelength absorbance detector

  - Alliance 2695 separation module, High performance liquid chromatographer

- 35mm x 10mm Petri plates; Sarstedt (Montreal, Quebec)
- C18 reverse phase column with polar end cap; Phenomenex (Torrence, California)
- CCF-STTG1 cell line; American Type Culture Collection
- FBS; Invitrogen (Burlington, Ontario)
- Alpha Mem; Princess Margaret Hospital (Toronto, Ontario)

2.2 Cell Culturing

Astrocytoma cells were grown from cryogenic storage (in α-Minimal Eagle Media (α-MEM with Dimethyl Sulphoxide (DMSO)) by thawing the cells, suspending them in 10ml of α- Minimal Essential Medium (α-MEM) supplemented with 10% (v/v) foetal bovine serum (FBS) and 1% (v/v) antibiotics in a $75cm^2$ collagen-coated flask. For 24 hrs, the cells were incubated in a thermoscientific incubator (Fisher) with 5% CO_2, set at 37º C in a humidified atmosphere. Past the 24 hr incubation, the culture medium was replaced with new medium so as to remove any remaining DMSO. The cells were then allowed to grow while being periodically checked until they reached confluency several days later. Upon reaching confluency, the culture medium was removed and prior to replacement, the cells were washed with phosphate buffered saline (PBS) [136.8mM NaCl, 2.5mM KCl, 1.83mM Na_2HPO_4, 0.4313mM KH_2PO_4 (pH 7.4)] to remove any old α-MEM as well as cellular debris. In order to passage the cells to a different flask, 10% (v/v) trypsin solution in PBS was used to cause the cells to detach from the collagen-coated flasks. Following a 2-3 minute exposure period to the trypsin and PBS solution, the trypsinization solution was

removed and α-MEM with 10% FBS was used to wash off the cells from the flask. The flasks were then hit against the palms in order to ensure that the cells are released from the collagen coat. The cells are then incubated for about 5 minutes after which they were passaged into new flasks at approximately 14 x 10^5 cells/ml. Cellular passaging was done from one flask to two flasks. Upon reaching confluency, the cells were then passaged from two flasks into five and four were used for experiments while the fifth was used to continue the cell culture (figure 10).

Stressing of the cells was accomplished by replacing the culture medium with serum-free medium. Prior to the replacement, the cells were washed with PBS to get rid of all cellular debris as well as any excess of the culture medium. To the four flasks, the stressors were then added: Lactate (2.5mM, negative control), Hydrogen Peroxide (4mM, positive control), 0.01mM Aluminum (0.01mM Al: 2.5mM lactate, Al stress 1) and 0.1mM aluminum (0.1mM Al: 2.5mM lactate, Al stress 2). The aluminum stressors were chelated to lactate to ensure optimal uptake by the astrocytes. The chelation was performed at a ratio of 1:5 so as to ensure that any cellular response observed was a metabolic one as opposed to a toxin avoidance response. A third of the batches were just stressed followed by isolation; a third were recovered for 24 hours with 1mM αKG and the final third were recovered for 24 hours with 1mM OAA.

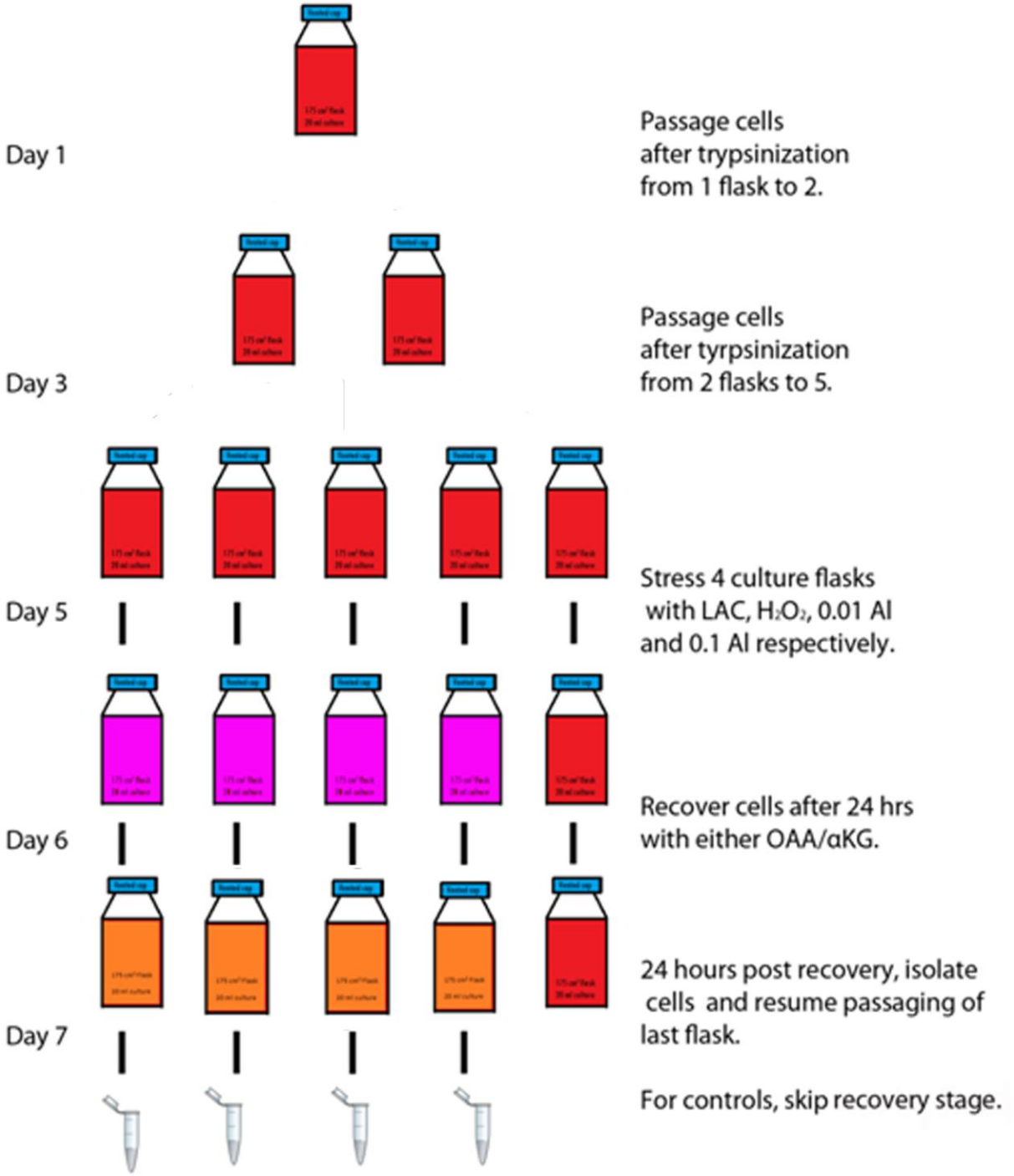

Figure 10: Overview of cell culturing

2.3 Cell isolation and spent fluid collection

Following a 24 hr period of stress and/or recovery with either of the two ketoacids, the culture medium containing the stressor (or ketoacid) was removed and the cells were gently washed with PBS. Aliquots of spent fluid were collected at each stage prior to washing the cells with PBS for metabolite analysis. Similar to cell passaging, the PBS was removed and the cells were then subjected to trypsinization to get them off the flask. Upon the detachment of the filopodia from the flask, the PBS containing the trypsin was removed and the cells were washed off using α-MEM. The α-MEM containing the cells, was then put into a 50ml conical flask and spun down at 2500rpm for 10 minutes at 4 ºC. The excess α-MEM was removed and the pellet was resuspended in 1ml of mammalian cell storage buffer (MCSB) (50mM Tris-HCl, 1mM phenylmethylsulfonylfluoride, 1mM dithiothreitol, 250mM sucrose, 1mg/ml of pepstatin, 0.1mg/ml leupeptine, 2 mM citrate) in an eppendorf tube. After being left in an ice bath for about five minutes, the cells were then stored in a freezer at -86 ºC. Samples of spent fluid collected were stored at -20 ºC.

2.3.1 Mitochondrial isolation

To isolate mitochondria, the cells were taken from storage at -86 ºC and thawed. The cells were then centrifuged at 400g for 10 minutes at 4 ºC. The spent fluid was then removed and the cells were resuspended in 100µL of MCSB with vortexing. Using a sonic dismembrator (Fisher), the cells were then homogenized at amplitude of 36% five times for 10 seconds each at one second intervals. The cells were then spun at 250g for 5 minutes at 4 ºC to ensure proper homogenization. Any left-over cells were then resuspended in 25 µL of MCSB and resonicated. The supernatants were then combined and spun down at 800g for 20 minutes at 4 ºC to obtain the nuclear fragments. The supernatant was taken and spun for

mitochondria at 12000g for 45 minutes at 4 ºC. The nuclear pellet was resuspended in 50 µL of MCSB and stored at -20 ºC. The mitochondrial pellet was resuspended in 50 µL of MCSB too and a Bradford assay was performed in triplicate to determine protein concentration.

2.4 Bradford Assay

Protein preparation for the Bradford assay was accomplished by adding 2 µL of isolated protein to 98 µL of 0.5 N NaOH for the mitochondrial fractions and 4 µL of the cytosolic fraction to 96 µL of 0.5N NaOH. The spectrophotometer cuvettes were then prepared as follows:

Table 1: Bradford assay

	Sample	Bradford reagent	ddH_20
Blank	0 µL	200 µL	800 µL
Standard	50 µL (200 µg/ ml BSA)	200 µL	750 µL
Sample	30 µL sample	200 µL	770 µL

Protein concentration is then calculated using the formula

$$[protein] = \frac{10\ x\ Average\ sample\ absorbance\ x\ dilution\ factor}{Standard\ absorbance\ x\ Volume\ of\ sample}$$

2.5 Native polyacrylamide gel electrophoresis

2.5.1 Sample preparation

The isolated CCFSTTG1 cells were diluted in a constant volume of 3x BN buffer (33.4 µL) and 10% (w/v) β- dodecyl-D-maltoside (10 µL) to a final concentration of 1mg/ml of protein and 1x BN buffer (50mM BisTris, 500mM 6- aminohexanoic acid, pH 7.0 at 4 ºC)

and 1% (w/v) maltoside. The prepared samples were then stored at -20 ºC and utilized within a week.

2.5.2 NATIVE Gel preparation

Bio-Rad MiniProtean™ II systems with 1mm spacers were used to prepare mini gels. In order to allow for the optimal separation of the proteins, a 4%-16% linear gradient was formed using a gradient former (Bio-Rad) and peristaltic pump (Fisher). Upon the polymerization of the running gel, the unit was overlaid with the stacking gel and the comb containing the wells for protein loading. Both the running gel and stacking gel were prepared as per the recipe given in table 2. The wells were then loaded with 30 µg of protein and overlaid with Coomassie Blue Cathode buffer (50mM Tricine, 15mM BisTris, 0.2g Coomassie Blue G250, pH 7 at 4 ºC). For molecular mass markers, bovine serum albumin (BSA) and ferritin were used. The inner chamber of the gel electrophoresis unit was filled with Coomassie Blue buffer and the outside chamber was topped off with anode buffer (50mM BisTris, pH 7 at 4 ºC). Upon assembling the electrophoresis apparatus along with the ladder and proteins to the electrophoresis unit, it was set at 80 V and 15mA and allowed to run until the end of the stacking gel. Once the protein reached the separating gel, the voltage was raised to 150 V and allowed to run till it reached the middle of the separating gel, at which time, the Coomassie Blue cathode buffer was removed and replaced with colourless cathode buffer (50mM Tricine, 15mM BisTris, pH 7 at 4 ºC). Once the running front reached the bottom of the gel, electrophoresis was stopped.

Table 2: Recipe for 4-16% BN-PAGE gel

	16% separating gel µL	**4% separating gel µL**	**½ Stacking gel**	**Stacking gel**
49.5% acrylamide	937	234	137	273
3X BN Buffer	967	967	568	1136
ddH_2O	223	1699	1000	2000
75% Glycerol	773			
TEMED	0.8	1	2.5	5
10% APS	7.6	9.7	15	30

2.5.3 In-gel enzyme assays and protein expression

After running the mitochondrial fraction through the gel, the gel was incubated in a 6ml reaction mixture (5mM isocitrate, 0.5mM NAD^+, 10% (v/v) INT and 5% (v/v) PMS) for approximately an hour. The reaction for the formation of αKG from isocitrate utilizes NAD to form NADH. As NADH goes back to NAD, it oxidizes the reaction of PMS^R to PMS^O. This reaction is coupled with the reaction of oxidized INT^O into its reduced form which precipitates to form a red coloration in proportion to the activity of the enzyme (figure 11).

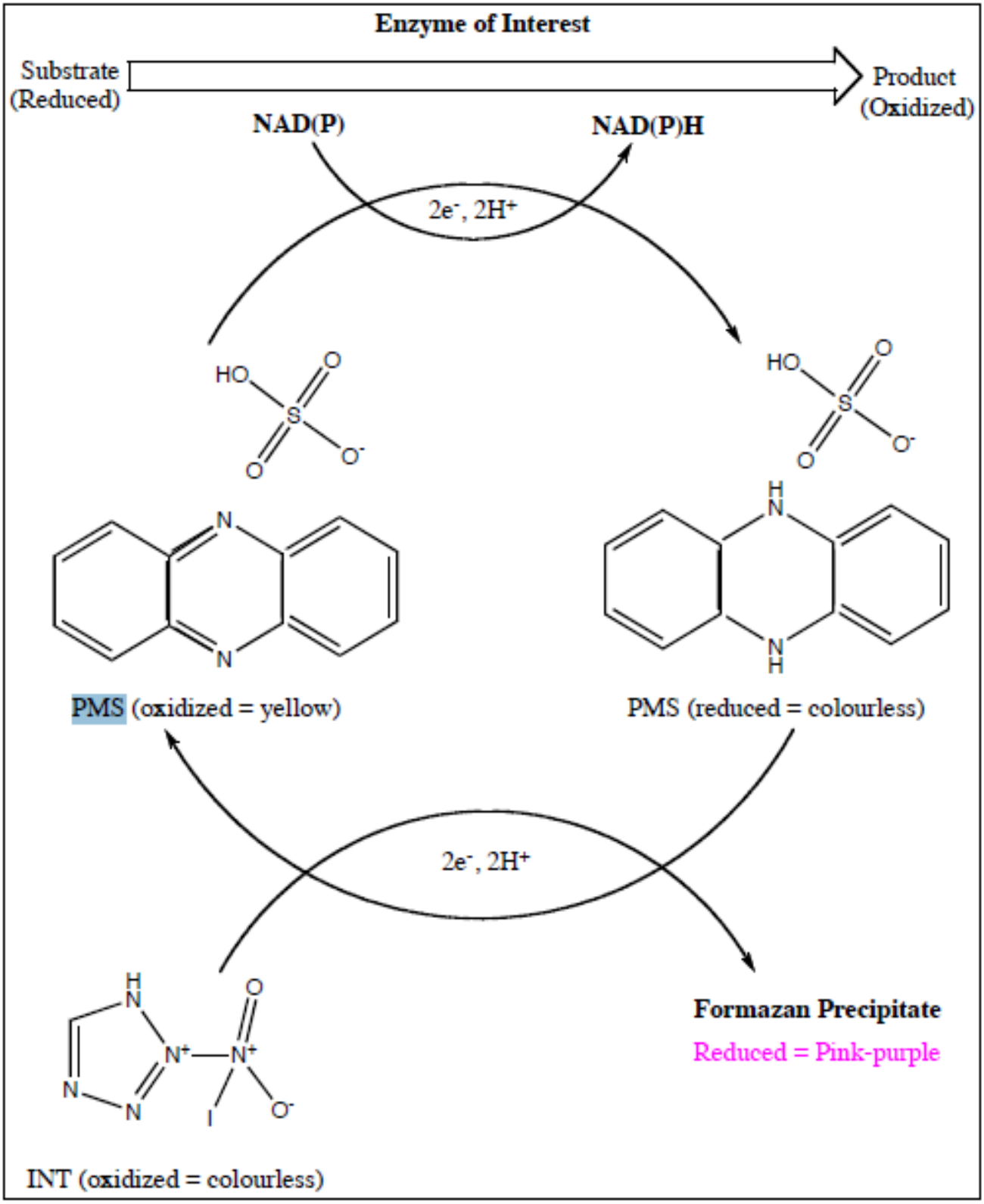

Figure 11: In-gel detection of NAD(P) dependent enzymes (Lemire, 2011).

2.6 Fluorescence microscopy

2.6.1 Culture growth

To gather cells for fluorescence microscopy, the CCFSTTG1 astrocytes were passaged from the 175cm^2 flask onto cover slips laid inside 35mm x 10mm Petri plates. The cells were then allowed a day for growth (70% confluency) prior to stressing. While stressing the cells on day two, a second set of astrocytes were passaged onto the cover slips. On day three, the first set of 4 cells that were stressed were recovered with either αKG or OAA and the second set were stressed. After an additional 24 hours, all cover slips were used to fix cells and prepare them for the fluorescence microscopy (figure 12). This ensured that we were able to compare NR cells to the ketoacid recovered cells.

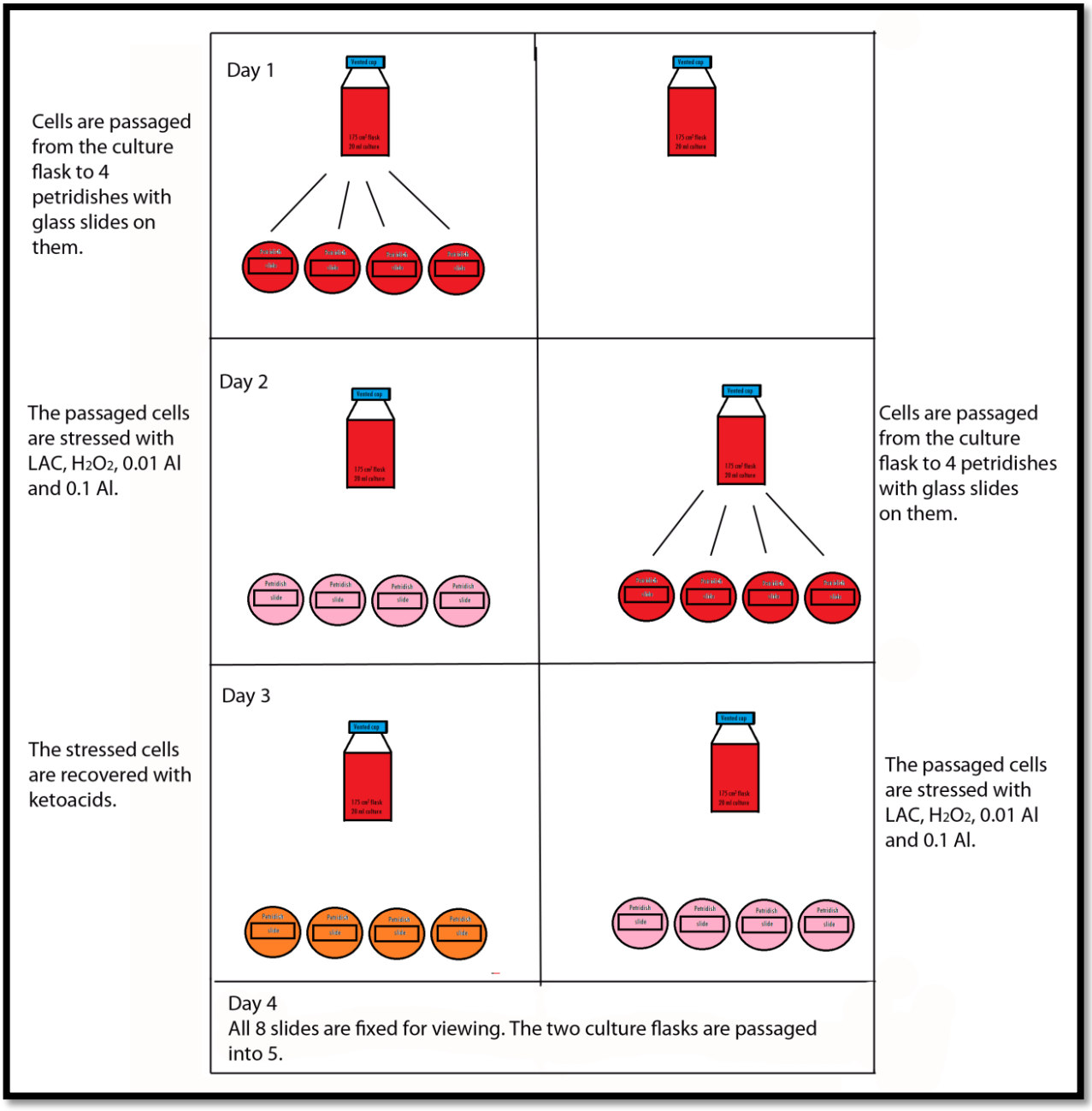

Figure 12: Overview of cell culturing for microscopy

2.6.2 Fixing the slides

24 hours after half the cells are stressed and the other half are recovered with ketoacids (after having been stressed for 24 hours prior), the cells were washed thrice with PBS. The slides were then fixed with a solution of 3:1 methanol and acetic acid for 10

minutes after which they were left briefly to air dry. PBS was used to wash the cells 2 more times and stained with Hoescht33342 stain (100 µL in 9.9ml of PBS) for 10 minutes. Upon removing the Hoechst stain, the cells were washed 3 more times with PBS and incubated with 2 ml of Oil Red O (0.25% w/v in isopropyl alcohol) for 10 minutes. For the DCFHDA stain, a 20 µM solution was used (DCFHDA in PBS) For the Rhodamine stain, a 1 µg/ml solution was used. The slides were then mounted with 10 µL of Permount (Fisher) mounting solution for observation. Using nail polish, the cover slips were sealed onto the microscopy slides and subsequently stored at -21 ºC until visualization which was accomplished using an inverted deconvoluted microscope (Zeiss). Axiovision software (Zeiss) was used to generate the merged images by simultaneously taking pictures of the two separate fluorophore channels.

2.7 High Performance liquid chromatography (HPLC) studies

High Pressure Liquid Chromatography (HPLC) was used in order to monitor the levels of malonate and succinate in the OAA recovered cells and αKG recovered cells respectively compared to NR cells. The cells were removed from storage at -86 ºC and thawed. Subsequently, they were broken open by sonication five times in the sonic dismembrator at 36% amplitude for 10 seconds at 1 second intervals with 5 minutes on ice between subsequent sonications. The cell free extract was then diluted in milliQ water and filtered into screw top sampling vials (Fisher) by making temporary filters using Pasteur pipettes patched with 1mm of cotton. The sampling vials were then loaded into the sample carousel of the HPLC (Waters Alliance 2695 separation module) and Empower software was used to program the injection protocol. Prior to the injection of samples into the HPLC column, the column was equilibrated with the appropriate mobile phase (20mM HPLC grade

KH_2PO_4 and milliQ water, pH 2.9) for 40 minutes. 20 µL of each sample was injected into the C18 reverse phase column (Phenomenex ®) with a polar cap, operating at a flow rate of 0.7ml/min at room temperature and a fluctuating pressure between 1000-1500 psi. Levels of organic acids were detected using a Waters model 2487 UV Vis dual wavelength detector operating at 210nm. Detection of carnitine levels was accomplished by collecting the flow through at a retention time of 4 minutes and rerunning it through the detector in a different mobile phase (20 mM KH_2PO4, pH 2.9 with 20% acetonitrile) at a flow through rate of 0.2ml/min. Pure samples were used as standards and the metabolite mixtures were spiked with the given metabolites to confirm peak identities.

Results

3.1 Lipid levels

The presence of intracellular lipid droplets was monitored using Oil Red-O staining as seen in figure 13. Cells stressed oxidatively and with aluminum appeared to contain the most lipids. However under all stress conditions, lipid levels were lowered and restored to normal under ketoacid recovery when compared to NR cells. For the lactate condition, there was no observable difference between the NR and αKG recovered cells but there appeared to be greater lipid accumulation in the OAA recovered cells.

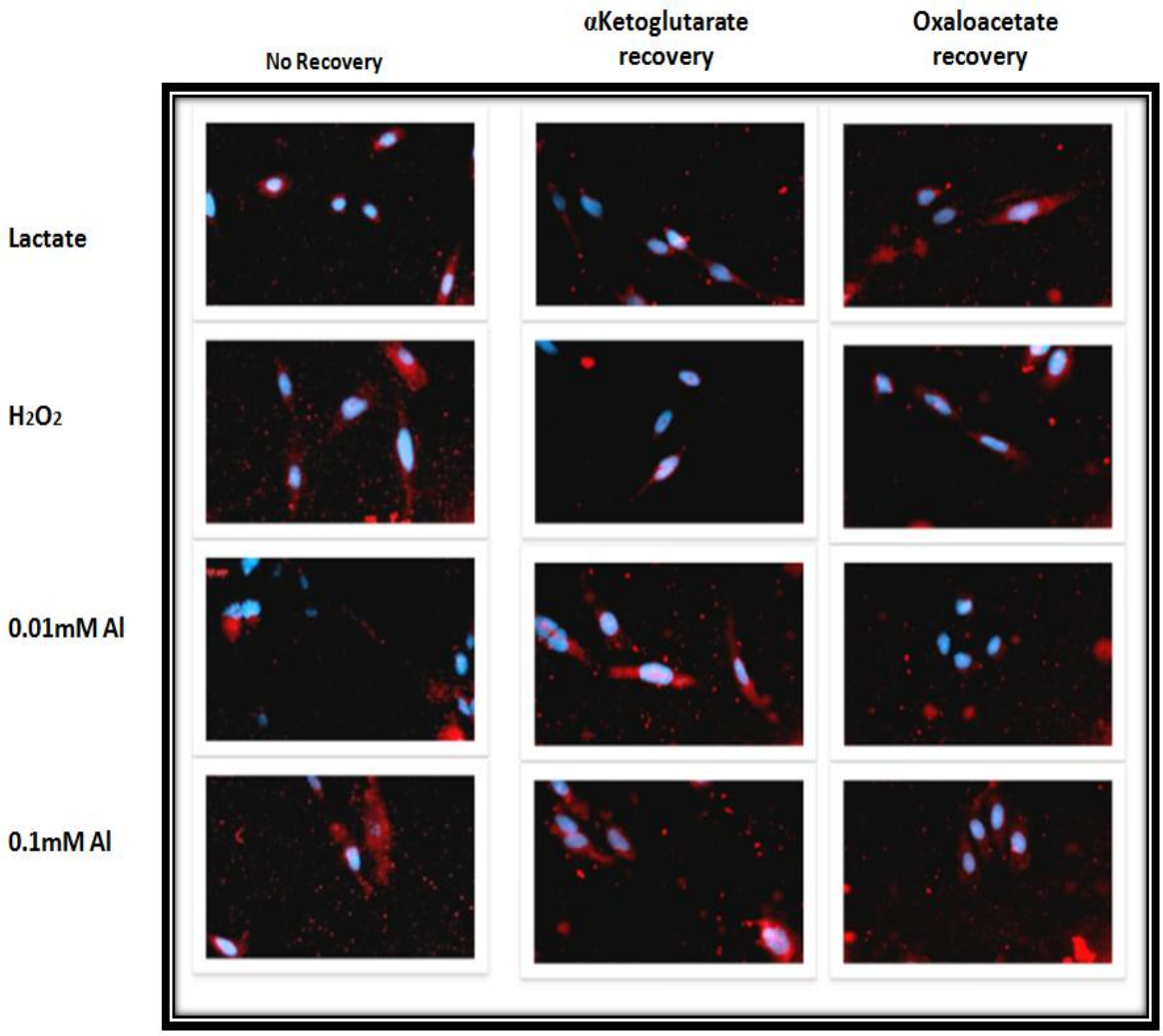

Figure 13: The astrocytes were stained with the Hoescht stain (nucleus-blue) and oil red-O stain (lipids-red). Fluorescence microscopy was performed at 20X ocular magnification. Overall, ketoacid recovery leads to reduction in lipid accumulation for the stress conditions.

3.2 Mitochondrial activity

The level of mitochondrial activity was assessed indirectly by measuring proton gradient levels within the cells using a rhodamine stain as seen in figure 14. Mitochondrial activity was found to be diminished under oxidative and aluminum stress and restored upon

recovery with OAA. Interestingly the control cells showed lowered mitochondrial activity upon recovery with OAA.

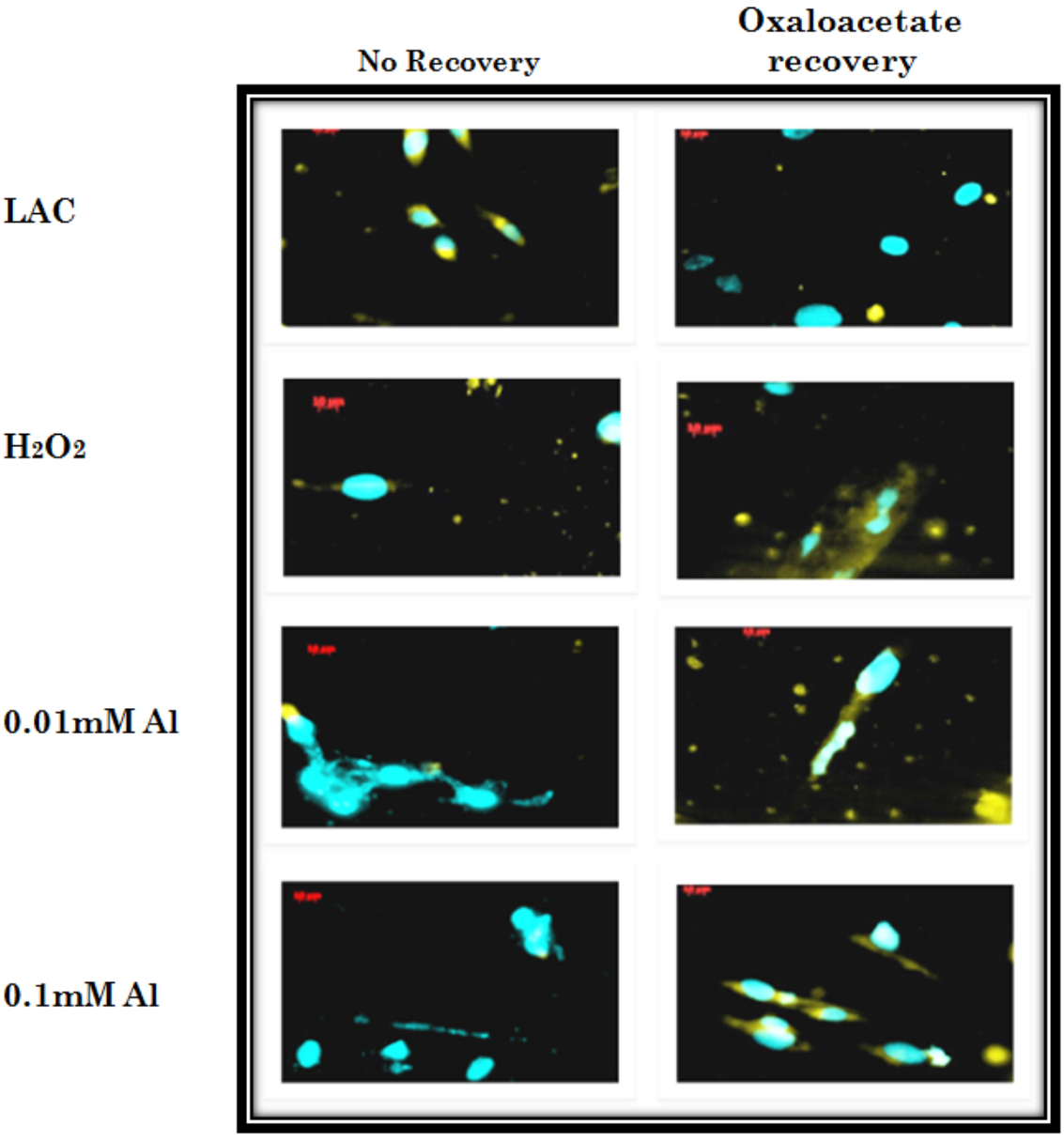

Figure 14: The astrocytes were stained with the Hoescht stain (nucleus-blue) and rhodamine (proton gradients- yellow). Mitochondrial activity was found to be consistently lower under stress but upon recovery with OAA was restored to normal.

3.3 Carnitine levels

Evaluation of the levels of carnitine within the cell free extract was performed for NR cells and OAA recovered cells using the HPLC and the results are shown in figure 15. Carnitine levels were lowest under 0.1mM Al stress for the NR cells. Although carnitine levels increased under all conditions of stress upon recovery with OAA, it only achieved statistical significance for the 0.1mM Al stress condition (All other conditions of stress were approaching significance ($p<.1$)). Interestingly for the lactate control, carnitine levels were significantly reduced upon recovery with OAA.

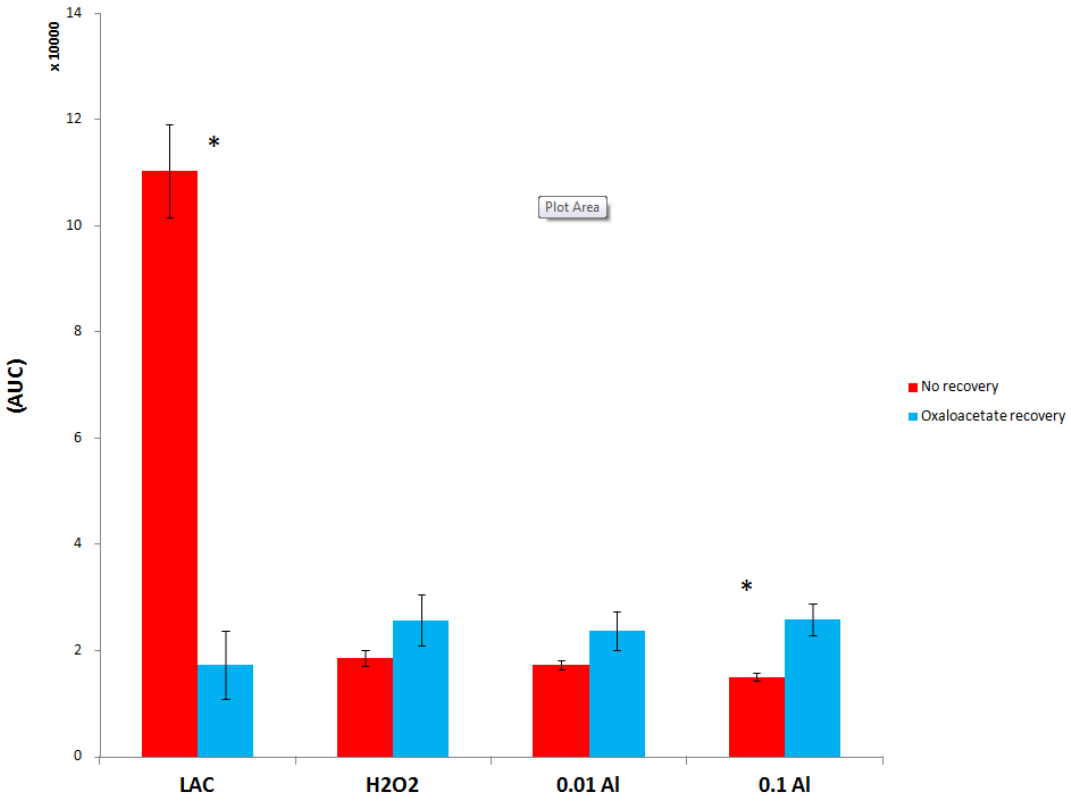

Figure 15: The cytosolic CFE for both NR cells and OAA recovered cells were used to monitor the levels of carnitine. The standard retention time for carnitine is 22 minutes. * marks significance at the $\alpha=.05$ level.

3.4 ROS Levels

The DCFH-DA staining of ROS showed greater presence of ROS in the cytosol of H_2O_2 and Al non recovered cells as seen in figure 16. In contrast, under conditions of OAA recovery, the levels of ROS were substantially lowered for the stressed conditions. No clear difference was seen for the control condition.

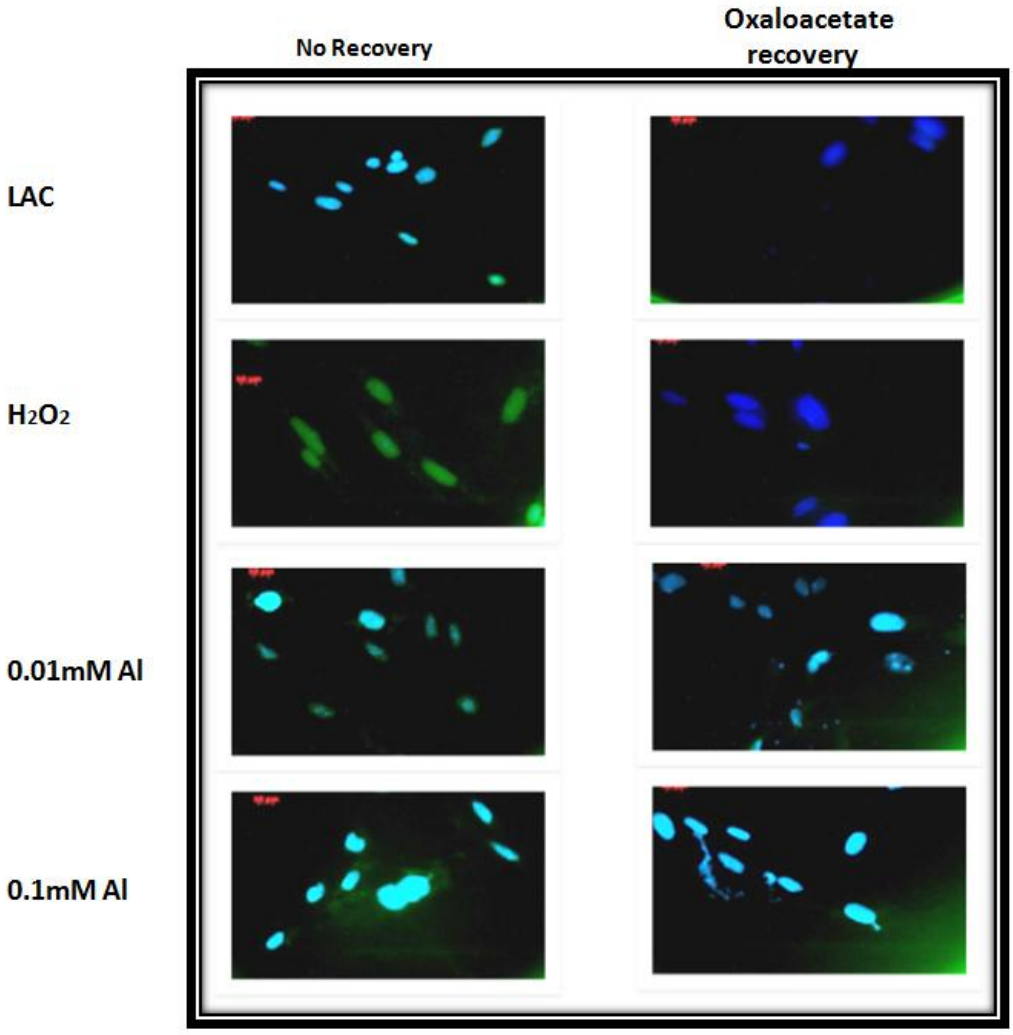

Figure 16: *The cells were stained with the Hoescht stain (Nucleus-blue) and DCFH-DA (ROS- green). Overall, ROS levels decreased under recovery with OAA when compared to the NR stressed conditions.*

3.5 Malonate levels

Evaluation of the levels of malonate within the cell free extract was performed for NR cells and OAA recovered cells using HPLC as seen in figure 17. Malonate levels were lowest under H_2O_2 for the NR cells. Malonate levels increased significantly over all when compared to the conditions of stress. However, it also increased significantly for the control.

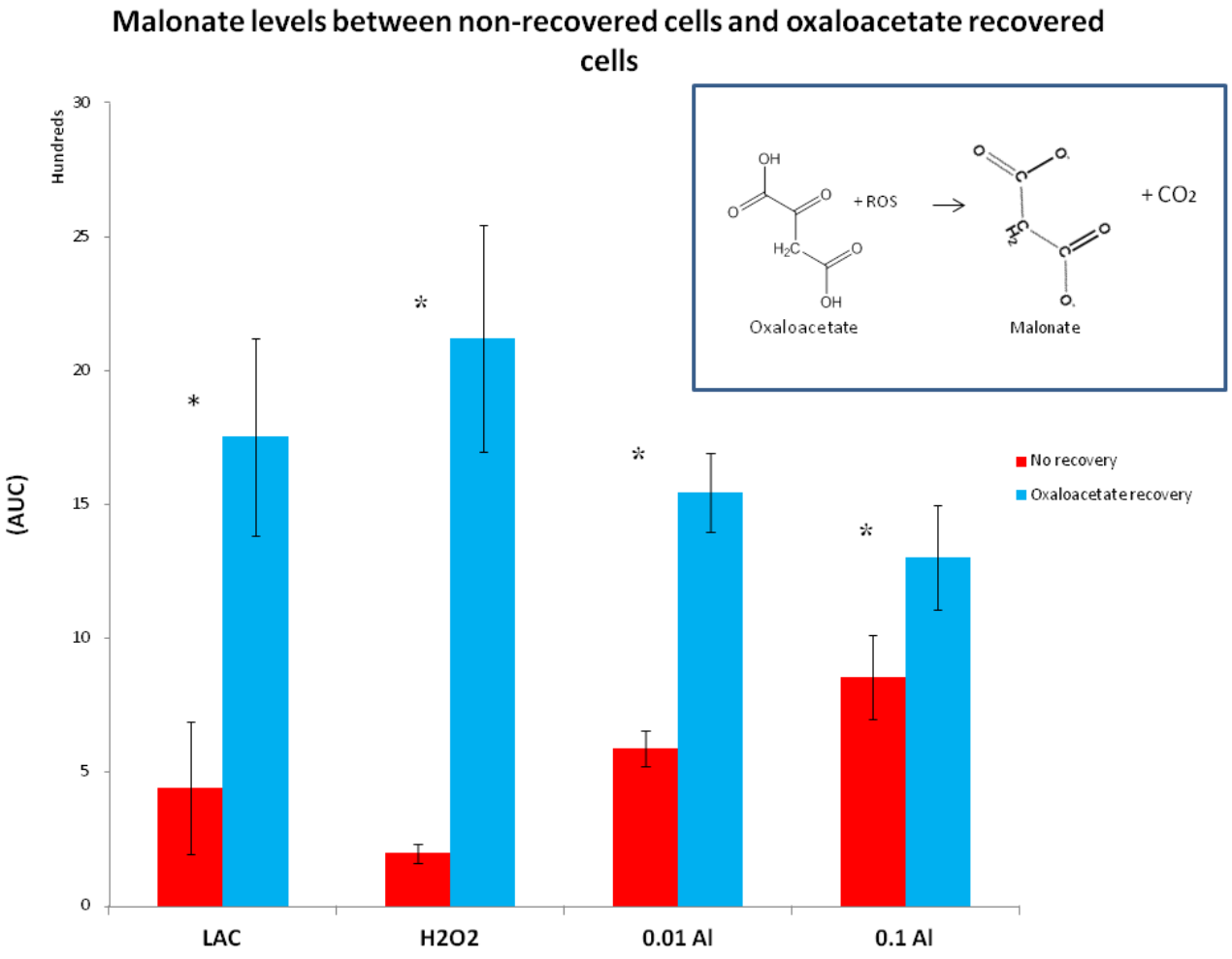

Figure 17: The cytosolic CFE for both NR cells and OAA recovered cells were used to monitor the levels of malonate. The standard retention time for malonate was 6 minutes. * marked significance at the α=.05 level.

3.6 Succinate levels

Evaluation of the levels of succinate within the cell free extract was performed for NR cells and αKG recovered cells using HPLC as seen in figure 18. Succinate levels were found to be lowest under the control condition for the NR cells and showed increases for all of the stress conditions. However the increases only achieved statistical significance for the 0.01mM Al condition. It is important to point out that the other conditions of stress were approaching statistical significance ($p<.1$).

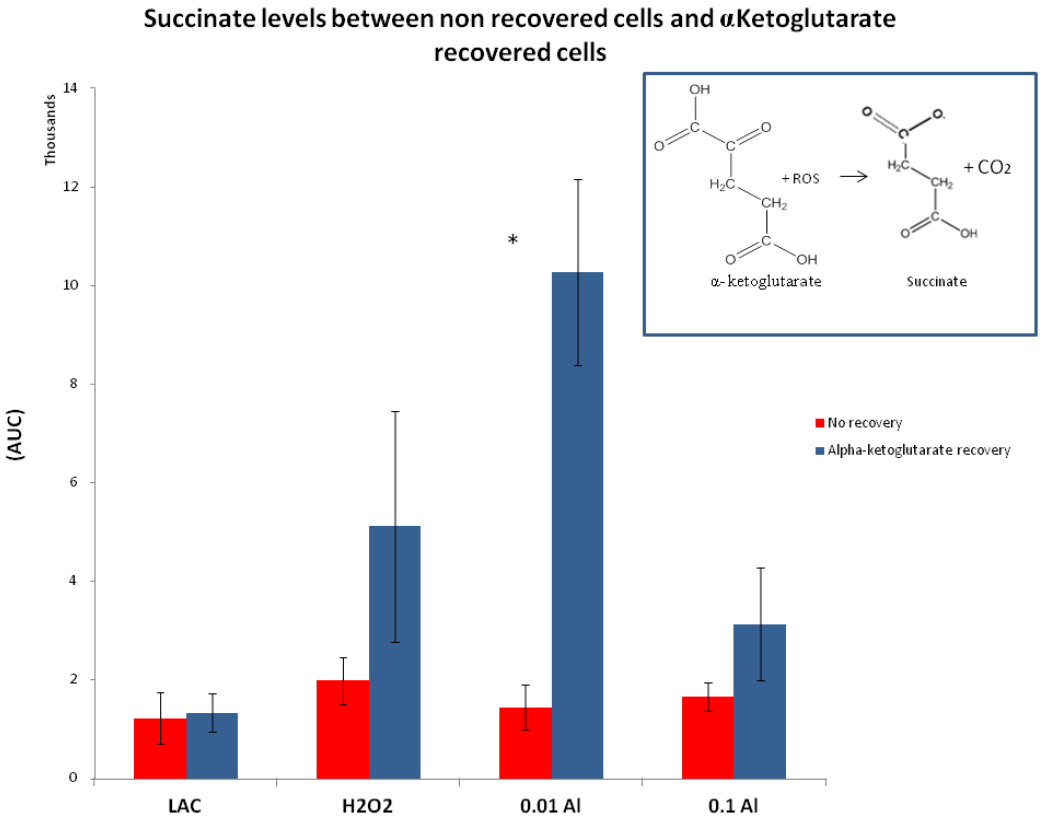

Figure 18: The cytosolic CFE for both NR cells and αKG recovered cells were used to monitor the levels of succinate. The standard retention time for succinate was 12 minutes. * marked significance at the $\alpha=.05$, level.

3.7 Blue Native Polyacrylamide Gel Electrophoresis for NAD-ICDH

The activity of NAD-ICDH, a key enzyme in the TCA cycle was assessed under native conditions as seen in figure 19. The relative activity of the NAD-ICDH isolated from the mitochondria was found to be down regulated under conditions of oxidative and aluminum stress as shown in previous research but as seen below, restored to normal when recovered with OAA.

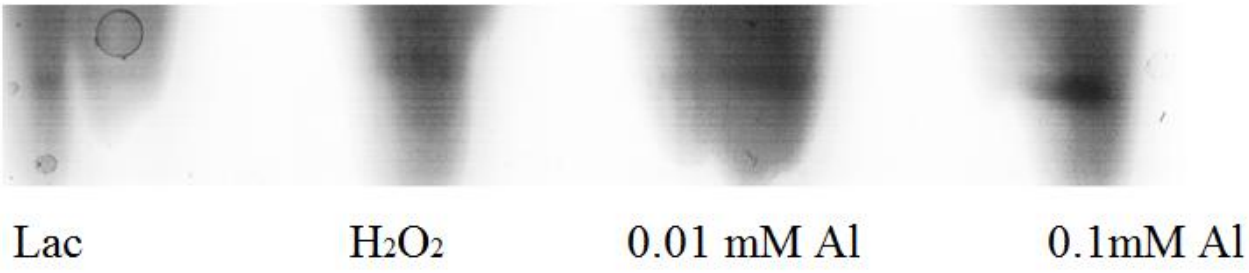

Figure 19: The mitochondrial fractions of both control and Al-stressed cells were separated under native conditions on a blue native polyacrylamide gel. The gel was then immersed in a reaction mixture to probe the activity of NAD-ICDH.

To confirm the presence of the enzyme, the bands were precision cut and stored in an Eppendorf tube containing the reaction mixture. At 5 minute intervals, the reaction mixture was taken out and analyzed by HPLC for isocitrate levels as shown in figure 20.

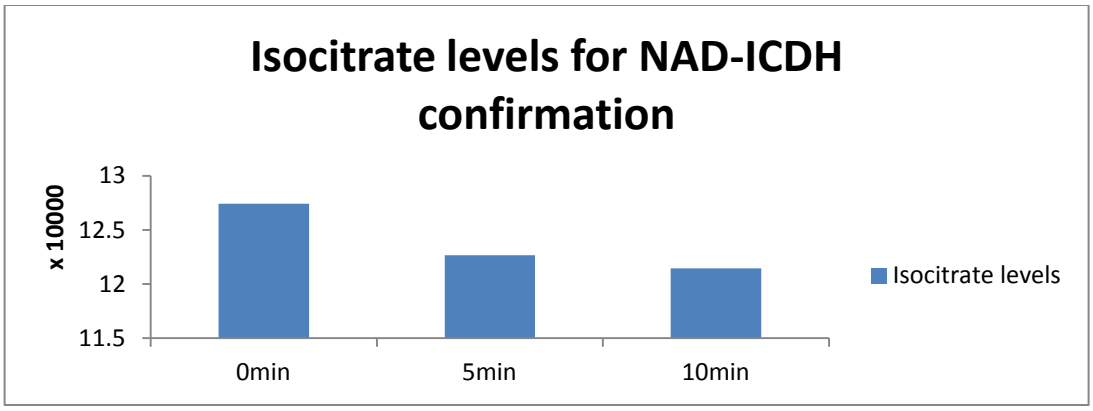

Figure 20: As time elapsed, the level of isocitrate was decreasing. NAD-ICDH catalyzes the reaction that utilizes isocitrate and forms αKG. The decreasing amounts of isocitrate across time, confirms that the bands did indeed possess NAD-ICDH.

3.8 Western blot for Apolipoprotein E expression

A western blot using Anti-ApoE antibody as the primary antibody and its appropriate secondary antibody with an infra-red tag, was used to assess the levels of apoE expression within the NR and OAA recovered cells as seen in figure 21. ApoE levels appeared to be diminished under aluminum stress but restored upon recovery with OAA.

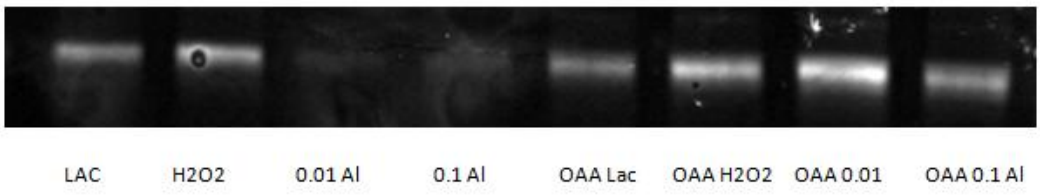

Figure 21: ApoE levels were assessed by doing a traditional western blot. The first 4 lanes represent the NR cells while the last 4 represent the OAA recovered cells. The bands showed up at the wrong molecular weight as measured using the Bio-Rad ladder on an SDS gel. Research suggests that this is probably due to the preventive action of lipid dissociation by the presence of β mercaptoethanol.

Discussion

Of the many important organs in the body, the human brain consumes the most energy in order to fulfill the energy requirements of its functioning in terms of action potential propagation. Thus, the brain tends to be highly vulnerable to ROS and as a result OS, both byproducts of the oxidative metabolism it undergoes. Among the various functions they perform, mature astrocytes can also detect OS in the brain and respond by undergoing reactive astroglyosis. In recent times, several neurological disorders have been associated with the presence of Al, a known pro-oxidant. Thus, current research is heavily focused on an attempt to delineate the role of Al in neurodegenerative disorders such as AD and PD (Smorgan et al, 2004). In the past, research has primarily been focused on the roles of Al and OS on neurons in relation to neurological disorders.

However, given that astrocytes perform a wide variety of critical roles such as scaffolding (Structural support), metabolic support, lipid metabolism and maintenance of neurotransmitter homeostasis, it is reasonable to expect that astroglial dysfunction would result in neurological dysfunction (Mailloux et al, 2007). However, increased anthropogenic acidification of soils, increased utilization of the metal in industry and the use of Al as a flocculent in water treatment has rendered it far more bioavailable and as a result is found to accumulate in living organisms including humans at a much greater rate than in the past (Lemire et al, 2011) As such, its toxicological effects have come under greater scrutiny.

To study the effects of Al and ROS and the role of ketoacids such as αKG and OAA, CCF-STTG1, a grade IV astrocytoma cell line was utilized. DCFH-DA stain was used to monitor ROS levels following 24 hours of stress (control, H_2O_2, 0.01mM Al(250 mM

Lactate) and 0.1mM Al(250mM lactate)) and subsequently 24 hours under recovery with either 1mM OAA. Under conditions of stressing with H_2O_2 as well as Al (0.01mM, and 0.1mM), the levels of ROS are substantially increased within the cytosol of the cells (figure 16) compared to the control. Recovery with 5mM αKG in previous research has demonstrated the ability of the ketoacid to lower ROS levels. Present research using 1mM OAA showed a similar trend wherein it resulted in a marked decrease in ROS levels. This result was expected since previous research using ketoacids as antioxidants has shown promise in other eukaryotic cell types (hepatocytes) as well as bacteria (*P. fluorescens*) (Mailloux et al, 2007) (Mailloux et al, 2006). Although this establishes the role of ketoacids as ROS scavengers, the mechanism through which this occurs is yet to be delineated.

αKG is known to undergo non-enzymatic decarboxylation by ROS to produce CO_2 and succinate (Fedotcheva et al, 2006). The increased utilization of αKG in combating ROS has been shown to have adverse effects in terms of lipid accumulation. Lemire et al. (2011) have shown carnitine levels to be decreased under conditions of oxidative and aluminum stress where αKG levels have been shown also to be markedly decreased and succinate levels highly increased. As demonstrated in figure 9, αKG is used in carnitine synthesis and carnitine is an important metabolite for transporting lipids into the mitochondria for beta oxidation.

By comparing succinate levels as seen in figure 18, it was observed that the succinate levels in the NR astrocytes under the given experimental conditions were found to follow the same trend as previously demonstrated in the literature (Lemire et al, 2011). Under recovery with αKG, succinate levels were shown to increase sharply in all conditions except

the control, which makes sense since the presence of ROS is required to facilitate the decarboxylation reaction.

Subsequently, malonate levels were analysed between the NR cells and OAA recovered cells. On top of its accumulation during ROS scavenging, malonate can play a very important role in energy supplementation. Malonate decarboxylase catalyzes the decarboxylation of malonate to acetate, a great source of complementary energy (Byun & Kim, 1994). Formation of malonate can occur through several pathways, of which the non-enzymatic decarboxylation reaction of OAA, to produce CO_2 and malonate, is the least energy demanding reaction, and thus most favourable. Interestingly unlike succinate levels, in the NR cells, the lowest malonate levels were consistently found under H_2O_2 stress. However under recovery with OAA, the highest malonate levels were also found for the H_2O_2 stress condition. Also of interest is the fact that malonate levels appeared to be significantly higher under OAA recovery for all experimental conditions including the control.

One of the adverse effects of oxidative stress as well as Al stress on astrocytes is their ability to halt oxidative metabolism and thereby decrease ATP production. This occurs due to the cells innate nature to try and limit the production of excess ROS. In astrocytes, this phenomenon was first shown by monitoring key enzymes such as NAD-ICDH, complex IV, etc. (Lemire et al, 2011). It was shown that under oxidative stress, NAD-ICDH activity was sharply diminished. Upon comparing the NAD-ICDH activity across conditions under OAA recovery, it was found that the activity is up-regulated in the stress conditions following OAA recovery. Taken in conjunction with the prior results, this makes sense because OAA helps scavenge ROS by undergoing the non-enzymatic decarboxylation to

form malonate. Thus since ROS levels have decreased, there is nothing inhibiting the occurrence of oxidative metabolism. Thus TCA cycle enzymes such as NAD-ICDH would be expected to be upregulated once more. In order to confirm the observations of the in-gel activity stain of NAD-ICDH, HPLC reactions were studied at varying time points after keeping the precision cut bands within the reaction mixture. NAD-ICDH catalyzes the reaction of isocitrate in the TCA cycle to form αKG. Thus over time, one would expect isocitrate levels to decrease if indeed the bands were NAD-ICDH. This was indeed found to be the case.

Previous research has shown in hepatocytes as well as astrocytes, that Al and OS tend lead to a decrease in ATP production through the disruption of the TCA cycle and ETC. (Mailloux et al, 2009). In an effort to scavenge and store energy for future use at a time when the conditions are more favourable, these cells resort to lipid accumulation as confirmed by the oil red O stains. However under recovery with ketoacids, the level of ROS decreases, thus providing the cells with a more favourable environment to continue with oxidative metabolism. Also αKG which is a precursor for the formation of carnitine which is used to transport lipids to the mitochondria for beta-oxidation, tends to get used up battling ROS. Thus, for the NR cells, a decrease in beta-oxidation is a key reason for lipid accumulation. However, under recovery with ketoacids, there are excess ketoacids for the battling and scavenging of ROS which allows for the rest to help with carnitine production and by extension beta-oxidation of lipids. As seen in figure 13, lipid levels for the NR cells showed similar results to previous research wherein lipid levels were highest under aluminum and oxidative stress. Comparatively, upon recovery with αKG as well as OAA, lipid levels were shown to be restored to normal for the stress condition. However for the

control condition, upon recovery with OAA, lipid levels were somewhat increased. In order to assess the mitochondrial activity, rhodamine staining was used as seen in figure 14. It confirmed the hypothesis that mitochondrial activity would be lowered under conditions of aluminum and oxidative stress. Although mitochondrial activity was shown to be restored in the stress conditions upon recovery with OAA, it was shown to be decreased upon recovery with OAA in the control condition.

Preliminary results showed that apolipoprotein E expression appears down-regulated under aluminum stress but not so much under control and H_2O_2 conditions. However recovery with oxaloacetate appears to restore expression levels to normal. The importance of Apolipoprotein E expression within the brain stems from its role in maintaining homeostasis of lipid metabolism and degradation of β-Amyloid which has been highly implicated in diseases such as AD and atherosclerosis. It appears as though Al directly affects apoE expression through some metal mediated pathway; an effect that is alleviated by the presence of OAA. The lack of down-regulation under H_2O_2 stress suggests that the mechanism of down-regulation of expression has to do more with the metal properties of Al than its oxidative stress effects.

Overall, for all conditions of oxidative and aluminum stress, the α-ketoacids, αKG and OAA were shown to help relieve ROS stress and restore lipid homeostasis and cellular functioning within the astrocytes. However while αKG showed no adverse effects in the control conditions, it was observed that OAA supplementation for the control cells showed most of the symptoms of OS including increased lipid accumulation, lowered mitochondrial activity, lowered carnitine levels and higher levels of malonate formation. Further

investigation has revealed that OAA is a potent inhibitor of complex II of the ETC (Huang et al, 2006). Thus in terms of therapeutic value, αKG shows more promise than OAA.

Conclusion

In conclusion, the results of this study confirmed the finding that lipogenesis is up-regulated as a result of OS and Al stress. This increase is likely mediated by the decrease in carnitine production as a result of lowered availability of αKG, a precursor to carnitine production. Studies have shown that OS and Al stress render the TCA cycle as well as the ETC highly dysfunctional. Thus energy production decreases which acts as the second prong towards ROS detoxification. Under recovery with αKG and OAA, these metabolites are utilized in ROS detoxification with the concomitant production of succinate and malonate respectively. Under these conditions of decreased ROS levels, the cells are able to resume normal oxidative metabolism and carnitine production for the utilization of lipids, thus restoring lipid levels to normal as well as restoring mitochondrial activity to normal. Under recovery with OAA, the TCA cycle was shown to be fully functional as gauged by the activity of NAD-ICDH in the mitochondria.

References:

Attwell, D., Laughlin, S.B., (2001) An energy budget for signaling in the grey matter of the brain. *J Cereb Blood Flow Metab. 21:*1133

Babior, B.M., (1999) NADPH oxidase: an update, *Blood 93:*1464

Barker, A.J., Ullian, E.M., (2010). Astrocytes and synaptic plasticity. *Neuroscientist 16:* 40

Coudray-Lucas, C., Le Bever, H., Cynober, L., De Bandt, J.P., Carsin, H., (2000) Ornithine alpha-ketoglutarate improves wound healing in severe burn patients: a prospective randomized double-blind trial versus isonitrogenous controls. *Crit. Care Med. 28*(6): 1772-6

De la Monte, S. M., & Wands, J. R. (2006). Molecular indices of oxidative stress and mitochondrial dysfunction occur early and often progress with severity of Alzheimer's disease. *Journal of Alzheimer's disease : JAD, 9*(2), 167181.

Fang, Y.Z., Yang, S., Wu, G., (2002). Free radicals, antioxidants, and nutrition. *Nutrition 18:*872

Fields, R.D. (2004) The Other Half of the Brain, *Scientific American 290*(4) , 54-61

Guzman, M., Blazquez, C., (2001) Is there an astrocyte-neuron ketone body shuttle? *Trends Endocrinol Metab 12:* 169

Herz, J., Chen, Y., (2006). Reelin, lipoprotein receptors and synaptic plasticity. *Nature 7:* 850-860

Huang, L.S., Shen, J.T., Wang, A.C., Berry, E.A., (2006) Crystallographic studies of the binding of ligands to the dicarboxylate site of Complex II, and the identity of the ligand in the "oxaloacetate-inhibited" state. *Biochim Biophys Acta 1757:*1073-83

Kim, Y.S., (2002) Malonate metabolism: Biochemistry, molecular biology, physiology, and

industrial application. *Journal of biochemistry and molecular biology 35(5):* 443-451

Kimura, Y., Kimura, H., (2004) Hydrogen sulfide protects neurons from oxidative stress. *FASEB J 18:* 1165

Lemire, J., Mailloux, R., Darwich, R., Auger, C., Appanna, V.D. (2011). The disruption of L-carnitine metabolism by aluminum toxicity and oxidative stress promotes dyslipidemia in human astrocytic and hepatic cells. *Toxicol Lett.*

Lemire, J., Mailloux, R., Puiseux-Dao, S., Appanna, V.D., (2009). Aluminum-induced defective mitochondrial metabolism perturbs cytoskeletal dynamics in human astrocytoma cells. *J Neurosci Res 87:* 1474

Lazarowski, E.R., Boucher, R.C., Harden, T.K., (2003). Mechanisms of release of nucleotides and integration of their action as P2X- and P2Y receptor activating molecules. *Mol Pharmacol 64:* 785

Magistretti, P.J., Pellerin, L., (1999) Astrocytes couple synaptic activity to glucose in the brain. *News Physiol Sci 14:* 177

Mailloux, R., Lemire, J., Appanna, V., (2007). Aluminum induced mitochondrial dysfunction leads to lipid accumulation in human hepatocytes: a link to obesity. *Cell physiol Biochem 20,* 627

Mailloux, R.J., et al, (2009). Alpha-ketoglutarate dehydrogenase and glutamate dehydrogenase work in tandem to modulate the antioxidant alpha-ketoglutarate during oxidative stress in Pseudomonas fluorescens. *J Bacteriol 191:* 3804

Mailloux, R.J., Hamel, R., Appanna, V.D., (2006). Aluminum toxicity elicits a dysfunctional TCA cycle and succinate accumulation in hepatocytes. *J Biochem Mol Toxicol 20:* 198

Martini, F., Ober, W.C., (2006) *Fundamentals of anatomy and physiology.* Pearson Benjamin cummings, San Francisco, CA, 7th ed.

Maalouf, M., Sullivan, P. G., Davis, L., Kim, D. Y., & Rho, J. M. (2007). Ketones inhibit mitochondrial production of reactive oxygen species production following glutamate excitotoxicity by increasing NADH oxidation. *Neuroscience, 145*(1), 2562-64.

Pfrieger, F.W., (2003) Outsourcing in the brain: do neurons depend on cholesterol delivery by astrocytes? *Bioessays 25:*72

Pertusa, M., GarciaMatas, S., Rodriguez, Farre, E., Sanfeliu, C., & Cristofol, R. (2007). Astrocytes aged in vitro show a decreased neuroprotective capacity. *Journal of neurochemistry, 101*(3), 794805

Raman, R, Pal, S.S., Adams, J.S., Rani, P.K., Vaitheewaran, K., Sharma, T., (2010) Prevalence and risk factors for cataract in diabetes l Sankara Nethralaya diabetic retinopathy epidemiology and molecular genetics study, report no. 17. *Invest Opthalmol Vis Sci. (12):* 6253-61

Schell, M.J., Molliver, M.E., Snyder, S.H., (1995) D-serine, an endogenous synaptic modulator: localization to astrocytes and glutamate-stimulated release. *Proc Natl acad Sci U S A, 92:*3948

Siegel, G.J., (2006) *Basic neurochemistry: molecular, cellular and medical aspects.* Elsevier, Amsterdam; Boston, 7th ed. Pp. xxiv, p. 992.

Varma, S.D., Devamanoharan, P.S., Ali, A.H., (1997). Formation of advanced glycation end (AGE) products in diabetes: prevention by pyruvate and alpha-ketoglutarate. *Mol cell Biochem 171*(1-2): 23-8

Walton, H. S., & Dodd, P. R. (2007). Glutamate glutamine cycling in alzheimer's disease. *Neurochemistry international, 50*(78), 1052-1066.

Yudkoff, M., Daikhin, Y., Melo, T. M., Nissim, I., Sonnewald, U., & Nissim, I.

(2007). The ketogenic diet and brain metabolism of amino acids: Relationship to the anticonvulsant effect. *Annual Review of Nutrition, 27,* 415430.

Zhu, X., Su, B., Wang, X., Smith, M. A., & Perry, G. (2007). Causes of oxidative stress in Alzheimer disease. *Cellular and molecular life sciences : CMLS, 64*(17), 2202-2210.